Vision Research 49 (2009) 2686–2704

Contents lists available at ScienceDirect

Vision Research

journal homepage: www.elsevier.com/locate/visres

Higher order color mechanisms: A critical review

Rhea T. Eskew Jr.

Department of Psychology, Northeastern University, Boston, MA 02115, United States

ARTICLE INFO

Article history:
Received 11 April 2009
Received in revised form 10 July 2009

Keywords:
Color
Higher order mechanism
Cardinal mechanism

ABSTRACT

A large number of studies, using a wide variety of experimental techniques, have investigated the "higher-order" color mechanisms proposed by Krauskopf and colleagues in 1986. Results reviewed here come from studies of chromatic discrimination at threshold, habituation, classification images, spatial alignment and orientation effects, and noise masking. The bulk of the evidence has been taken to support the existence of multiple, linear color mechanisms in addition to (or after) the three putative low-level cardinal mechanisms. But there remain disconcerting inconsistencies in the results of noise masking experiments, and the results of chromatic discrimination experiments clearly show that there are a very limited number of labeled-line mechanisms near threshold. No consensus on higher order mechanisms has been reached even after more than 20 years of study.

1. Introduction

The modern psychophysical concept of "mechanism" was first applied to the photoreceptors (Graham, 1989; Stiles, 1949) and its explanatory power derived mainly from information loss. Because Stiles' π mechanisms were assumed to be univariant, responding in the same way to each photon regardless of its wavelength, the psychophysicist did not have to account for chromatic detection at myriad wavelengths, but instead could attempt to reduce the problem to the spectral sensitivities of the π mechanisms, of which there were eventually eight.

The lack of correspondence between the π mechanisms and the photoreceptors, especially as revealed in failures of psychophysical mechanism properties such as field additivity (Pugh & Kirk, 1986), led to the demise of Stiles' model. The color vision scientist no longer speaks of photoreceptors as abstract mechanisms, the functional consequences of their physiological properties now being so well established that the abstraction is no longer needed. Instead, the mechanism concept has been taken additional steps inside the visual system, to post-receptoral levels, with the idea of explaining aspects of color vision beyond those that can be attributed to the activities of photoreceptors. However, the goal has been similar to the early modeling of photoreceptors: to simplify color vision by positing a limited number of abstract, theoretical entities – mechanisms – to attempt explain a range of phenomena. This paper reviews some developments in color vision over the past quarter century, focusing on questions about the number and nature of color mechanisms. Related material may be found in recent reviews by Eskew (2008) and Stockman and Brainard (in press).

2. Cardinal axes

By the mid-1980s, a substantial consensus had developed on the outlines of a model of color detection and discrimination. LeGrand (1949/1994) had analyzed MacAdam's (1942) chromatic discrimination ellipses and shown that their variation seemed largely explicable in terms of two chromatic variables, one a difference of the *L* and *M* cone signals, the other the *S* cone signal. Rodieck (1973) took a similar approach. Boynton and Kambe (1980) made extensive new discrimination measurements along these "theoretically critical" axes. Then, in 1982, Krauskopf, Williams, and Heeley (1982) published a paper that was to become extraordinarily influential, in which they referred to these chromatic axes (plus a "luminance" axis) as the "cardinal directions" of color space. These threshold results were superficially consistent with models of hue (Hurvich & Jameson, 1957), at least in so far as that they required some form of chromatic opponency to explain the data. This work, and more like it, led to a model of the sort shown in Fig. 1a (Boynton, 1979; Lennie & D'Zmura, 1988).

The model has three mechanisms or channels. One is based upon a difference of outputs of the *L* and *M* cones, with no input from *S* cones. *A* second mechanism takes the difference between *S* cones and an additive combination of *L* and *M* cones, and the third mechanism is based upon a sum of *L* and *M* cone signals. The outputs of the mechanisms are bipolar – they may either exceed or fall below their adapted level (double-headed arrows). The weights of the cones are implicitly given as unity in the drawing, but this is not a defining characteristic of the model, as various relative weightings would be consistent with much of the data at that time. The key point is that the cone signals are combined as a weighted sum.

E-mail address: eskew@neu.edu

0042-6989/$ - see front matter © 2009 Elsevier Ltd. All rights reserved.
doi:10.1016/j.visres.2009.07.005

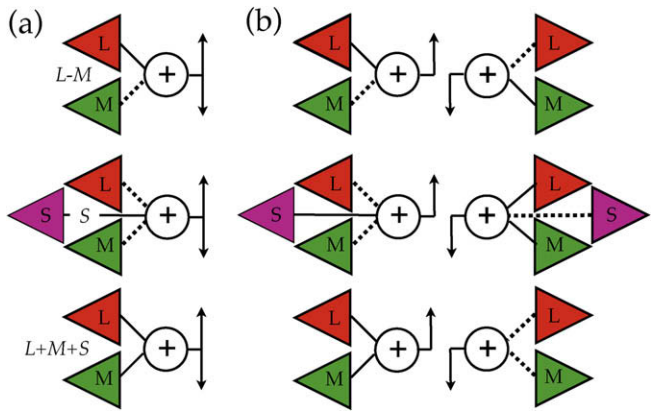

Fig. 1. (a) The cardinal model. The three cone types combine linearly into three postreceptoral mechanisms. Dashed lines refer to sign-inversions of signals. At the top, the $L - M$ mechanism takes the difference between L and M cone signals. In the middle, the $S - (L + M)$ mechanism is formed from the difference of the short-wave cones and a weighted sum of the two long-wave cone types. At the bottom, the luminance mechanism sums outputs from L and M cones, with no contribution from S cones. In each of the three rows, the letters in italics refer to the cone modulations that, because they do not stimulate the other two mechanisms, are the isolating color directions for the mechanism in that row. These are thus the cardinal axes. (b) The two poles of the each part of (a) have been split into rectified, unipolar mechanisms. The direction the output arrows point is arbitrary.

In Fig. 1b, the two poles of each bipolar mechanism have been rectified into two separate mechanisms. Because the two halves are symmetric (the three cone weights are of opposite signs but equal magnitudes, and the directions of maximum responsivity are complementary), this variation on the cardinal mechanism model makes identical predictions to Fig. 1a model for *stimuli* that are bipolar and symmetric, such as grating patches, flicker, or noise. Giulianini and Eskew (2007) refer to mechanisms that are linear except for half-wave rectification as "half-wave linear" mechanisms. In the discussion below, the term "cardinal" will be used to refer to either of the models in Fig. 1.

3. Higher order mechanisms

In a second extremely-influential paper, Krauskopf, Williams, Mandler, & Brown, 1986 reanalyzed the original data for cardinal mechanisms, as well as presented new data, and found evidence for what they termed "higher-order" color mechanisms, conceived of as recombinations of signals from the cardinal mechanisms, and tuned to color directions that are intermediate between cardinal axes (such as 'orange' or 'blue–green'). There are two aspects to this idea, which are logically separate: first, that there are additional – multiple – mechanisms beyond the cardinal ones, and second, that these exist at some higher level of the visual system. Virtually all of the psychophysical data bears only on the first aspect, the number of mechanisms.

The second, "higher level" part of the concept is often addressed not by psychophysical experiments, but by reference to the results of physiological studies. Many of the papers reviewed below begin by citing psychophysical experiments, but then quickly turn to physiology to justify speculations about the level of the psychophysical mechanisms in the processing stream. However, it is not yet clear even which cortical areas are most relevant for color. Moreover, the large number of feedback connections from various cortical regions to one another, and back to lateral geniculate, call into question the idea that there is an anatomically-definable (as opposed to functional) hierarchy. It is the prejudice of the present author that, given the difficulties posed by these issues in our present state of knowledge, a psychophysical concept like "color mechanism" must be justified by psychophysical experiments, and therefore this review focuses exclusively on perceptual data. A few remarks on cortical physiology, and the "higher" aspect of "higher order" mechanisms, will be made in later sections. To keep the terminology consistent with most of the papers on this topic, the term "higher order" will be used here even though "multiple mechanisms" or "non-cardinal mechanisms" might be more apt.

Evidence for higher order mechanisms has been obtained from studies of detection (D'Zmura & Knoblauch, 1998; Gegenfurtner & Kiper, 1992; Gunther & Dobkins, 2003; Krauskopf et al., 1986; Lindsey & Brown, 2004), classification images (Bouet & Knoblauch, 2004; Hansen & Gegenfurtner, 2005), first-order discrimination (Hansen & Gegenfurtner, 2006; Krauskopf, 1999; Krauskopf & Gegenfurtner, 1992; Li & Lennie, 1997; Zaidi & Halevy, 1993), and second-order (texture) discrimination (Goda & Fujii, 2001; Li & Lennie, 1997). Other tasks providing such evidence include visual search (D'Zmura, 1991; Monnier & Nagy, 2001; Nagy, Neriani, & Young, 2004), spatial alignment (McGraw, McKeefry, Whitaker, & Vakrou, 2004; McKeefry, McGraw, Vakrou, & Whitaker, 2004), detection of Glass patterns (Cardinal & Kiper, 2003; Wilson & Switkes, 2005), motion coherence (Krauskopf, Wu, & Farell, 1996), tilt aftereffect and tilt illusion (Clifford, Spehar, Solomon, Martin, & Zaidi, 2003; Flanagan, Cavanagh, & Favreau, 1990), and color appearance (Krauskopf, Zaidi, & Mandler, 1986; Mizokami, Paras, & Webster, 2004; Webster & Mollon, 1991, 1994). The diverse nature of the tasks makes it unlikely that each is limited by a common set of chromatic "mechanisms", or indeed that each is limited by mechanisms at a particular level of processing, and so this review will emphasize the simpler and better-understood tasks such as detection and discrimination. These studies, and others, provide substantial evidence against the simplest model of color mechanisms (as shown in Fig. 1); the unsettled question is whether a different model might account for the same phenomena without positing a large number of mechanisms.

4. Color representations

Most of the studies discussed here represent their data in some variation of the color spaces described by MacLeod and Boynton (1979) and Derrington, Krauskopf, and Lennie (1984), which will here be called MBDKL space. Cone excitations (quantal or energy catch rates) in the three cones are first converted to local coordinates by subtracting the adapted baseline or background excitations from the excitation produced by the test modulation (e.g., $\Delta L = L_{\text{test}} - L_{\text{adapt}}$). The three local cone excitations are rotated, such that the axes of MBDKL space are $\Delta L - \Delta M$, ΔS, and $\Delta L + \Delta M + \Delta S$, but with the delta symbol normally suppressed (Krauskopf, 1999). These three axes are the "cardinal" directions of Krauskopf et al. (1982), designated by the cone modulations that putatively isolate the mechanisms, not the cone modulations that most efficiently stimulate them (Eskew, McLellan, & Giulianini, 1999; Knoblauch, 1995; Krauskopf, 1999). The isolating cone modulations are shown in italics in Fig. 1a.

Spherical coordinates are often used in MBDKL space, with the azimuth giving the angle in the equiluminant plane (axes $\Delta L - \Delta M$, ΔS), and elevation specifying the projection onto the luminance axis. In the equiluminant plane, 0° usually refers to a reddish L-cone increment and M cone decrement, 180° to the greenish complement, and 90° and 270° to S-cone increments and decrements, respectively.[1] Some authors use the putative mechanism inputs (e.g., $S - (L + M)$) to label the axes (e.g., Hansen

[1] However, in some papers, this axis is inverted: the 90° azimuth indicates the S-cone decrement (yellowish) direction (e.g., Krauskopf et al., 1982) (Hansen & Gegenfurtner, 2005).

& Gegenfurtner, 2006), rather than the isolating direction labels (*S*). The magnitudes of MDKL coordinates are arbitrarily related to one another, and so threshold scaling is often used to specify angles and distances.

An alternative representation is cone contrast space, with axes that are the local cone excitation coordinates (e.g., ΔL) divided by the adapted baseline or background excitation (e.g., $\Delta L/L_{adapt}$ or simply $\Delta L/L$). Cone contrast space incorporates a simple version of cone-independent adaptation (von Kries adaptation). Cone contrasts are dimensionless and need not be further normalized.

As discussed later, all the studies reporting evidence favoring higher order color mechanisms have represented data in MDKL or a similar cone excitation space. All the studies failing to find such evidence have used another representation, such as cone contrast space.

5. Color mechanism: a provisional definition

Before discussing the data on higher-order mechanisms, it seems obviously important to define what is meant by a "mechanism", although very few papers on this topic offer explicit definitions. Here, a chromatic detection mechanism is defined as a fixed (relative) combination of cone signals that is correlated with the observer's behavior in psychophysical experiments (Eskew, 2008). Mechanisms are assumed to be stochastically independent at threshold. There is no need to require mechanisms to be orthogonal in any particular color space, nor indeed must mechanisms be assumed to be linear combinations of cone signals. The cone signals are combined in the mechanism postreceptorally, meaning that first-site, cone-specific adaptation has already occurred. This cone-specific adaptation may be approximated by use of cone contrasts, but other models of that adaptation could easily be substituted. Manipulations such as masking or habituation (reviewed below), or facilitation due to pedestals or edges (Cole, Stromeyer, & Kronauer, 1990; Eskew, 1989; Eskew, Stromeyer, Picotte, & Kronauer, 1991; Gowdy, Stromeyer, & Kronauer, 1999), which act at the mechanism output, change overall sensitivity but not chromatic tuning.

Two additional assumed properties of mechanisms make strong predictions about chromatic discrimination. First, "univariance" implies that when two stimuli are detected by one and only one mechanism, there is some relative intensity at which the two stimuli cannot be discriminated from one another. Second, the "labeled line" assumption (Graham, 1989; Watson & Robson, 1981) implies that when two stimuli are detected by different mechanisms, they must be discriminable from one another at all relative intensities. These discrimination assumptions have important implications. For example, since "red" and "green" stimuli, and *S* increment and *S* decrement stimuli, can be discriminated from one another at detection threshold, under conditions where a single mechanism is isolated (Eskew, Newton, & Giulianini, 2001; Krauskopf et al., 1986; Mullen & Kulikowski, 1990), these stimuli are detected by different mechanisms, by definition. While the cone inputs may act antagonistically within the mechanism (they may be *cone*-opponent), the mechanism cannot be perceptually *color*-opponent, because qualitatively different outputs must be associated with different mechanisms, according to these two assumptions. Although there are cells at early levels of the visual system that have bipolar responses, the responses of later cells that are surely the substrate for psychophysical mechanisms must be rectified in some way (although rectification alone is insufficient to account for chromatic habituation and other data – see Zaidi & Halevy, 1993 for discussion). These considerations mean that the model depicted in Fig. 1a does not satisfy this definition of 'mechanism'; that of Fig. 1b does. This rectification is an important aspect of the color model of De Valois and De Valois (1993).

It may be that some of these mechanism properties do not apply to higher-order mechanisms. Take, for example, the assumption of a fixed relative spectral sensitivity. It could only be realistic when first-site adaptation is taken into account, since it is very clear that there is cone-specific adaptation and that does alter relative spectral sensitivity (Eskew et al., 1999; Stockman & Brainard, in press).[2] The assumption of fixed relative spectral sensitivity is quite restrictive, and could exclude adaptive networks that might be very important for higher-level vision. However, relaxing the fixed relative spectral sensitivity assumption too readily would make it difficult to reject any model: almost anything could be explained if mechanism tuning could change arbitrarily. A principled approach that does relax this assumption, 'adaptive decorrelation' (Atick, Li, & Redlich, 1993; Zaidi & Shapiro, 1993), will be briefly discussed later. Univariance and labeled lines may similarly be too restrictive. However, the theoretical approach taken here is to explicitly make these simplifying assumptions, and reject them only if the data require it.

6. Rationale of the experiments

The logic of many of the experiments described below is as follows: some effect (such as masking or habituation) is studied as a function of the chromaticity of two stimuli. Call one the test, the other the auxiliary stimulus. The test is set to some color direction, and the color angle of the auxiliary stimulus is varied. To be concrete, imagine a detection task with the auxiliary stimulus being masking noise (Gegenfurtner & Kiper, 1992; Giulianini & Eskew, 1998; Hansen & Gegenfurtner, 2006). In old-fashioned terms, this is a field sensitivity experiment (Stiles, 1978), in which changes in sensitivity to the (constant chromaticity) test are used to index the sensitivity to the auxiliary or field stimulus (however, in many applications of this logical approach something other than thresholds are measured). In comparison, a test sensitivity experiment, less diagnostic (Stockman & Brainard, in press) and less-frequently used, involves variation in the stimulus being detected under fixed adaptation conditions. Sometimes the test and field sensitivity methods are used in combination, such as when threshold detection contours (test sensitivities) are measured in the presence of masking noise at various color angles (field sensitivities; e.g., combining all the panels of Fig. 6).

Most of these experiments restrict stimuli to one plane of color space. The auxiliary stimulus (e.g., noise) angle is varied relative to the test color angle, and the main features of interest in the resulting profile of sensitivity are: (a) the location of the peak – does the color angle of the largest effect of the auxiliary stimulus coincide with the test color direction, or is it elsewhere? (b) what is the shape, and particularly the bandwidth, of the masking pattern?; (c) at what color angle does the field sensitivity fall to zero – is this at a color angle that is 90° away from the test color angle? If mechanisms are nonlinear, there are no general predictions. If there are many *linear* mechanisms, then the answers should be: (a) the peak effect should be at or near the test, no matter what the test is, because the test direction is similar to a mechanism direction; (b) the shape should be approximately a cosine (Derrington et al., 1984) and (c) when the auxiliary stimulus is at right angles to the test it should have little effect, again no matter what the test angle. If there are a limited number of linear mechanisms, then the answers are similar (Webster & Mollon, 1994), but the peak may not be at

[2] Cone-specific adaptation is the only nonlinearity prior to cone combination mentioned here, but the mechanism concept could easily be extended to include other nonlinearities, both before and after the site cone combination.

the test direction but rather the closest mechanism direction (Krauskopf et al., 1986).

The details can matter: for example, noise masking effects are linear in the square of the noise contrast, not contrast (Gegenfurtner & Kiper, 1992), and so the bandwidth of threshold elevation is slightly narrower than the 60° of a cosine (Eskew, 2008). If the test does not isolate a single mechanism, so that its unmasked threshold is reduced by probability summation among the mechanisms that are sensitive to it, then the putting the auxiliary stimulus at right angles to the test may not lower its threshold all the way to the unmasked baseline, since the orthogonal noise may mask at least some of the mechanisms that were sensitive to the no-noise test; indeed in noise masking studies the orthogonal noise often has a small masking effect on non-cardinal tests (e.g., Hansen & Gegenfurtner, 2006 Ð see the present Fig. 7). If performance in the task required some complex and nonlinear processing of visual inputs, then a deviation from a simple mechanism prediction might have nothing to do with color, but rather with the poorly-understood cognitive demands of the task. For this reason this review emphasizes tasks that are closely tied to chromatic aspects of the stimulus, and for which there are relatively simple models linking putative mechanism output with observed performance. Even with that restriction, the reader should keep in mind that the link between model output and threshold is not the same as between model output and orientation judgment, for example.

The experimental logic outlined above has been employed in many of the studies reviewed below. In addition to the noise masking experiments, the same basic logic is used for habituation and detection (Krauskopf et al., 1986), habituation and color appearance (Webster & Mollon, 1994; Webster & Wilson, 2000), pedestal masking (Krauskopf & Gegenfurtner, 1992), tilt induction and adaptation (Clifford et al., 2003; Flanagan et al., 1990), Glass pattern detection (Cardinal & Kiper, 2003; Wilson & Switkes, 2005), and visual search (Nagy et al., 2004). As will be demonstrated in one specific case (Fig. 14), this logic is not completely secure; non-orthogonal and nonlinear mechanisms can produce maximal effects at the test direction and minimal effects 90° away, if not for all tests then at least for many of them, without having a large number of mechanisms.

Other approaches, such as chromatic discrimination experiments, have a different logic, based upon the univariance and labeled line assumptions described above. That logic is described later, in Section 11.

7. Habituation

In their "cardinal axis" paper, Krauskopf et al. (1982) used adaptation to 1 Hz frequency flicker, which they referred to as 'habituation' (and Webster and Mollon (1991) call 'contrast adaptation'). Observers viewed 30 s of flicker along some color direction before attempting to detect a single Gaussian pulse of color, either along the habituating direction or some other. Fields were 2° spots with no surround. Habituating to flicker along a cardinal axis raised thresholds on that axis, and had little effect on the orthogonal test axis; this was taken as strong evidence for the cardinal axis model. However, a later re-analysis of the data, using a clever application of Fourier analysis to average data across conditions, revealed a pattern in the results suggesting there were additional mechanisms: maximum habituation occurred at each test angle, not just at the cardinal axes (Krauskopf et al., 1986). The results of habituation along non-cardinal directions were very much second-order and somewhat inconsistent effects on thresholds; the primary effect was habituation along the cardinal axes.

Webster and Mollon (1991) and Webster and Mollon (1994) used asymmetric color matching to study the effects of habituation in the equiluminant plane (and more limited measurements in other planes). Fig. 2 shows the basic idea. The filled circles represent the chromaticities of the square test patch. Observers adapted the region of the retina where the test was shown to 1 Hz sinusoidal flicker along a particular color axis (the example shows 135°/315°). Like Krauskopf et al. (1982), amplitudes were equated to be the same multiple of threshold at different color angles. The open symbols represent the chromaticity of a matching patch, presented to unadapted retina, for each of the test colors. The schematic shows three of the main features of the results: (a) the maximum adaptation (difference in radius at a given angle) occurred when the test and adapting stimulus were on the same color direction, and this was true for intermediate as well as cardinal axis adaptation; (b) the minimum effect of adaptation was when the test was orthogonal to the adapting direction, again whether or not the adapting modulation was along a cardinal axis; (c) the adaptation rotated the matching stimulus, indicating a change in hue, except along the adapting axis; for other test colors, the hue changes were generally rotations away from the adapting axis, towards the orthogonal axis. Webster and Wilson (2000) combined adaptation to steady (DC) backgrounds with contrast adaptation and extended the earlier results to a wider set of conditions.

The simple cardinal axis model of Fig. 1 could not account for the effects of habituation on threshold or on asymmetric color matching, assuming that habituation acts independently within each mechanism to simply scale sensitivity at the output. Webster and Mollon (1994) discussed two approaches to modifying the theory to account for these results: a more complex type of mechanism, or a large number of simple mechanisms, could be postulated. An example of the former approach is an 'adaptive decorrelation' algorithm (Atick et al., 1993; Zaidi & Shapiro, 1993), which could alter the gains in post-receptoral mechanisms, following habituation. The model accounts for the asymmetric color matching of Webster and Mollon (1994) by decorrelating the cardinal mechanism outputs, rotating the pattern of matches as in

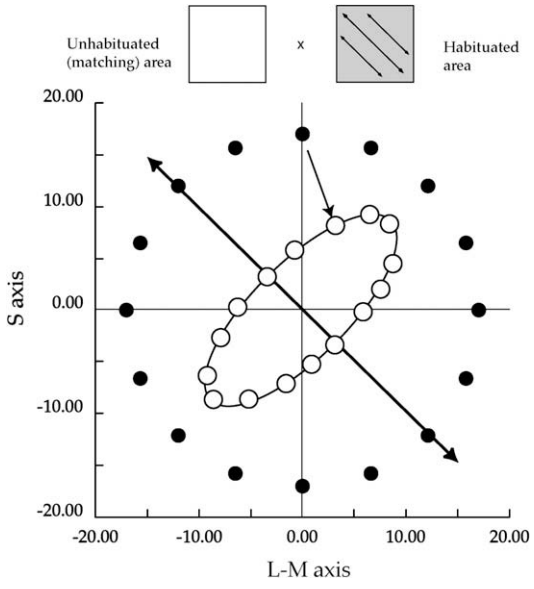

Fig. 2. Schematic representation of the effect of habituation on asymmetric color matching, based upon Webster and Mollon (1994). The two rectangles represent the matching and standard stimuli, presented on either side of fixation. The observer is habituated to modulations at a particular color angle (arrow, bottom). The filled symbols represent the standard stimuli, from various angles in the equiluminant plane. The open symbols represent the chromaticity of the match after habituation. The maximum effect of habituation is at the habituating angle, and the minimum is 90° away. Note that the *S* cone stimulus is no longer matched by an *S* cone test.

Fig. 2. Adaptive processes like this violate one of the assumptions in the definition of color mechanism given earlier, because the relative spectral sensitivity of a mechanism is not fixed (and not as the result of cone-specific adaptation), but they could in principle account for Webster and Mollon's result without adding multiple mechanisms. Webster and Mollon (1991) considered adaptive decorrelation but favored the multiple mechanism model.

It is natural to consider adaptive decorrelation a high-level process, as the algorithm takes cardinal mechanism responses as its inputs. On the other hand, there is no obvious reason that multiple linear mechanisms tuned to various color directions must exist at a high level of the visual system. Nevertheless, both theoretical approaches would generally be classed as "higher order" models. A theme of this review is that there are two possible approaches to altering the cardinal model to account for experimental results: adding additional simple mechanisms (as in Fig. 12, below), or adding complications, such as nonlinearities and asymmetries, to a limited set of mechanisms (as in Fig. 13, below). The adaptive decorrelation idea could be viewed in the second category.

8. Classification images

Hansen and Gegenfurtner (2005) and Bouet and Knoblauch (2004) used variations on the classification image technique (Ahumada, 2002). In the Hansen and Gegenfurtner study, an equiluminant colored rectangle, with chromaticity at one of the four cardinal directions or the four intermediate ones, was embedded in a noise texture composed of samples from across the equiluminant plane. Using standard methods, the authors computed the difference of: (a) the average of the noise patterns that were present when the observer responded that the target was present and (b) the average of the noise patterns that were present when the observer responded that the target was absent, separately for each test chromaticity. This classification image shows the average of the noise patterns that influence the observer to see the target, revealing the sought-after features (colors). Fig. 3 shows a depiction of three of their classification images. The main results were that the classification images had an ill-defined spot, centered on the test rectangle, that was similar in color to the target, and that this was true whether or not the target was on a cardinal axis (the 0°, $L-M$, and 90°, S-panels) or an intermediate axis (the 45° panel). The authors interpreted this result as the result of the action of higher order mechanisms, so that the noise pattern that most influenced detection had a color similar to the target being sought, including not only the cardinal directions but the non-cardinal ones as well.

Bouet and Knoblauch (2004) worked in the temporal rather than spatial domain. Random flicker, with chromaticities drawn from the target chromatic axis and the orthogonal axis, was added to a Gaussian test pulse. The added noise waveforms were classified and averaged according to the decision of the observer, and two sorts of classification images were computed. In the first type, the noise was decomposed into its two chromatic direction vectors, which were analyzed separately. When the noise component along the target direction alone was used, a Gaussian waveform, similar to the actual test waveform, was obtained. When the orthogonal axis noise alone was used, the result was flat, indicating no temporal variation in the influence of the orthogonal component on detection; this was true for the intermediate as well as cardinal test directions. However, modeling showed that the cardinal axis model could account for this result.

In the second analysis of Bouet and Knoblauch, the two noise chromatic axes were combined rather than analyzed separately; like Hansen and Gegenfurtner's (2005) spatial classification images, the waveforms of Bouet and Knoblauch (2004) had chromaticities similar to the target, even for the intermediate target chromaticities.

Both sets of authors (Bouet & Knoblauch, 2004; Hansen & Gegenfurtner, 2005) interpreted their results as showing that there are mechanisms tuned to all the tested directions, including the intermediate ones. However, in fact the cardinal axis model (Fig. 1) – or simple variations of it, as described in Section 13 – predict the same agreement between test color and classification image even for the intermediate test colors. The intermediate targets are detected by one cardinal axis mechanism on some trials, by the other on other trials, and by both on some trials. The chromatic "features" that should most efficiently trigger these detections are the chromaticities along the two cardinal axes. The result of pooling these trials would be a classification image pattern representing the average of the two cardinal axis chromaticities – which is the intermediate color axis where the test was located – exactly as found in both of these studies. Thus the results of these classification image studies do not distinguish between the cardinal mechanism and higher order models.

Hansen and Gegenfurtner (2005) also analyzed their classification data in terms of the influence that each noise chromaticity had on their observers' hits, false alarms, misses, and correct rejections. Plotted as a function of chromatic angle in the equiluminant plane of MBDKL space, these 'color histograms' were presented as a way of estimating the chromatic tuning bandwidths of the underlying detection mechanisms. The color histograms can also, in principle, address the question of whether intermediate tests were detected by cardinal mechanisms. On the grounds that the peaks of these histograms roughly aligned with the test color (but with some systematic deviations, and narrower bandwidths for non-cardinal compared with cardinal tests), the authors inferred the presence of higher order mechanisms. Unfortunately, however, Hansen

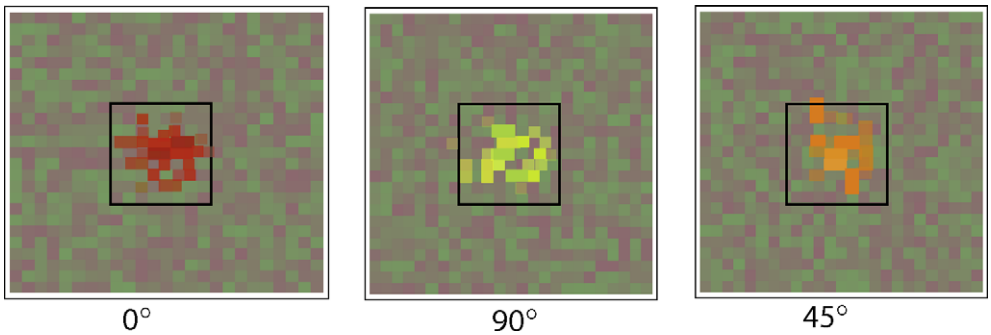

Fig. 3. Representations of classification images from Hansen and Gegenfurtner (2005). In each panel, the black rectangle outlines the actual test region. The colors represent the chromaticities that were correlated with the observers' decisions when looking for tests in the equiluminant plane a 0° (red), 90° (yellowish, the S cone decrement), or 45° (orange).

and Gegenfurtner did not present a quantitative argument to exclude the possibility that the cardinal-mechanism model could produce a similar pattern of results. And, indeed, simulations by the present author suggest that the cardinal axis model does produce peak 'color histogram' values near the test angle even for non-cardinal tests, and bandwidths that depend strongly upon the observer's criterion level. Consequently, the color classification results, while impressive, may not distinguish cardinal-like models from higher order ones. Further discussion is beyond the scope of this review.

9. Alignment and orientation effects

McGraw et al. (2004) used an interesting positional adaptation technique. Observers were adapted to two odd-symmetric patches (first derivatives of Gaussians), vertically arranged in a column, then tested with a column of three even-symmetric (Gaussian) patches, at the same two positions as the adapting patches plus the central position. A sample of their stimuli is shown in Fig. 4. This adaptation can produce a shift in the apparent position of the central Gaussian test (Whitaker, McGraw, & Levi, 1997). In this example, adapting to a pair of white (left)-black (right) elements can cause the middle white Gaussian blob to appear out of line, to the left. McGraw et al. (2004) measured the amount of perceived shift in the central element, based upon the chromaticities of the test and adapting patches in the equiluminant plane. The result that the maximum shift came when the test chromaticity was the aligned with one of the two chromaticities in the adapting pattern, and the minimum occurred when orthogonal to those chromaticities. This was true for all tested adapting chromaticities, not simply the cardinal ones. The authors argued that this was evidence for multiple chromatic mechanisms. Some of the tuning functions (shift in perceived location as a function of angle in the chromatic plane, for a given adapting stimulus) were narrow, which the authors modeled with a cosine raised to a power greater than 1.0, symmetrically narrowing the tuning (D'Zmura & Knoblauch, 1998).

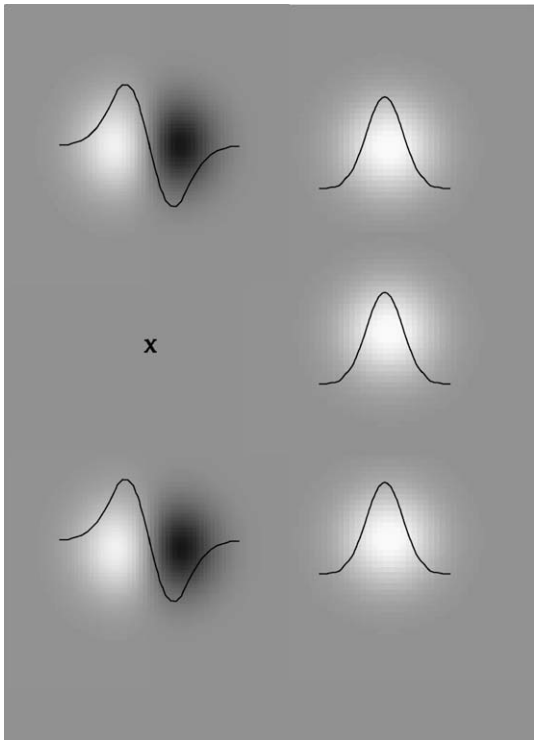

Fig. 4. Example stimulus arrangement, using achromatic patterns, from the positional adaptation experiment of McGraw et al. (2004). The observer fixates between the two odd-symmetric patterns on the left. When the pattern on the right is then viewed, the middle element appears shifted laterally.

Flanagan et al. (1990) studied the tilt aftereffect produced by gratings of various chromaticities. In the main condition, observers were exposed to high-contrast gratings, tilted 15° off vertical, that alternated between one color (with one tilt) and another color (with the other tilt). After the adapting period, a vertical test grating was shown, and observers used a matching procedure to indicate the perceived tilt of the test. Adapting gratings were always separated by 90° in a plane of cardinal axes space; the equiluminant plane, and also two planes including the equichromatic axis, were used. Test gratings were sampled at 22.5° intervals around the plane under study.

The main result was that maximum tilt aftereffects were obtained along the cardinal axes, with effects varying roughly sinusoidally with color angle. The design of the experiment, with oppositely-tilted gratings pitted against one another, means that the minimum effect was obtained midway between the two adapting gratings (a minimum at 45° color difference, not 90°). For example, a red/green and an *S* cone adapting gratings at (0° and 90° in the equiluminant plane) could induce maximal, oppositely-tilted aftereffects on 0° and 90° tests, with little effect for an intermediate test (at 45°). This was true for the equichromatic as well as equiluminant gratings. The authors argued that this supported the existence of adaptable, orientation-tuned cardinal axis mechanisms. However, adapting gratings at color angles intermediate to the cardinal axes (e.g., purplish/greenish at 45° and teal/orange at 135°) produced similar, albeit smaller, aftereffects, with a maximum when the test was at the intermediate color angle and no effect when the test was along a cardinal axis. The authors attributed this to additional, non-cardinal mechanisms. In a second condition, using a single adapting grating, evidence for non-color selective oriented mechanisms was found as well, and with the single grating the common maximum effect at the test color direction, and minimum effect 90° away in color space, was found.

More recently, Clifford et al. (2003) studied orientation and color using simultaneous tilt induction. An annular surround grating, tilted ±15° off vertical, induced a measured apparent tilt into a central grating patch. Maximal tilt induction was found when the two patterns were on the same color direction, and it did not matter whether that was a cardinal or non-cardinal axis. However, the tilt illusion did not drop to zero for orthogonal color axes; the tuning of the effect in color space had a narrow peak and broad, non-color selective flanks.

In both these tilt effect papers, the stimuli were quite large (especially in Clifford et al. (2003), where the inducing annulus had inner and outer diameters of 3° and 15°), and one might be concerned about retinal inhomogeneity producing multiple 'mechanisms' at different stimulus locations. However, Flanagan et al. (1990) took several steps to minimize chromatic aberration, and both studies used 1 cycle per degree gratings, which should minimize luminance artifacts.

Glass pattern detection offers an intriguing possibility for studying higher order perceptual effects of various kinds, although colored Glass patterns present some technical challenges. In these experiments, a "signal" set of randomly arranged elements is superimposed on a displaced copy of those elements, generating a large number of pairs of elements forming a characteristic moire' pattern, whose detectability may be reduced by the addition of additional uncorrelated "noise" elements. Wilson and Switkes (2005) used patterns whose elements were dots with blurred edges, to minimize effects of chromatic aberration, placed within a 7.4° circular window. Chromatic variations were either between dot pairs (interdipole) or within (intradipole) them. The latter case is of particular interest here, since oriented receptive fields would

have to pool across different chromaticities in order to provide the basic orientation 'front end' that is believed to underlie Glass pattern detection (Dakin, 1997).

Wilson and Switkes (2005) equated equiluminant color contrast by finding the contrast that yielded the same coherence threshold (35% coherent dot pairs) when the pattern was composed entirely of dots of a single color. Then they selected a reference chromaticity – say, 0° (red) – and varied the chromaticity of the dots making up the oriented (signal) dipoles. The results were that when the second dot chromaticity was 90° away from the reference, the observer could no longer detect the Glass pattern; the bandwidths for the fall-off in coherence threshold were near 50° (narrower than a cosine), and it did not make a great deal of difference whether the reference color was along a cardinal axis or was intermediate. This study of intradipole color varation is consistent with there being multiple higher-order mechanisms that are orientation-tuned.

Both Wilson and Switkes (2005) and Cardinal and Kiper (2003) also studied the coherence threshold for Glass patterns in which the dots within the signal pairs were of the same chromaticity, but there were noise dots of a different chromaticity (interdipole variation), to examine possible longer range interactions. The results were rather different in the two studies. Cardinal and Kiper (2003), who used very large (20°) dot patterns with contrasts arbitrarily set across chromaticities, found very broad tuning, with maximum thresholds obtained for noise chromaticities roughly similar to the signal chromaticity, and with minima that were very roughly 180° away (in other words, the best performance was obtained when signal and noise dots were complimentary). Wilson and Switkes (2005), on the other hand, found essentially no tuning: the chromaticity of the noise made no difference to the coherence. These results with interdipole color variation might suggest that long-range spatial pooling occurs across color mechanisms in Glass pattern detection, but it is not clear that they bear on the number or nature of the color mechanisms themselves.

10. Detection in noise

Noise masking has been the technique that has been most widely applied to the study of higher order color mechanisms, beginning with Gegenfurtner and Kiper (1992), who embedded Gabor and square patches in two-dimensional dynamic random noise, and studied threshold elevation for targets in the plane of the ($L - M$, equichromatic) axes. They found evidence for multiple, narrowly-tuned detection mechanisms. Threshold elevations were maximal near the test direction even for tests intermediate between cardinal axes, and narrower than a linear mechanism prediction.

Conflicting reports have followed this pioneering chromatic noise making experiment. Sankeralli and Mullen (1997) and Giulianini and Eskew (1998) found evidence for linear, broadly-tuned mechanisms more similar to the cardinal mechanisms. Working in the (L, M) plane, Giulianini and Eskew (1998) put Gaussian blobs or Gabor patches in randomly flickering lines or rings. Fig. 5 shows data from one observer. The left panel shows a detection contour for a Gabor patch without noise (open symbols), and with approximately-equiluminant red/green flickering rings superimposed over the tests (filled symbols); these are test sensitivity data. The noise shifts the long, unit-sloped flanks (straight lines through open symbols) outward substantially, while having much less effect upon the threshold at 45°, centered between the two lines.

The authors interpreted these results as showing that the noise masked a red/green mechanism that weights its L and M cone inputs with opposite sign but equal magnitude, creating the unit-sloped detection contours (e.g., Cole et al. (1990); see Eskew et al. (1999) for a review). Stimuli falling along those unit-sloped lines cannot be discriminated from one another at threshold, whereas stimuli on different line segments can be perfectly discriminated (Eskew et al., 2001; Newton & Eskew, 2003), as discussed further in Section 11, and the outward shift of that segment of the detection contour indicates a desensitization of that mechanism without a change in relative spectral sensitivity.

According to the model, the threshold at 45° was detected via an achromatic or luminance mechanism; when the approximately-equiluminant red/green noise was added it had little effect on that mechanism, but reduced the sensitivity of the red/green mechanism and exposed more of the luminance mechanism (the negatively-sloped contour segments). The threshold color appearance of the tests near 60–80° changed from greenish without noise, when they fall along the positively sloped contour segment, to achromatic with noise, when they fall along the negatively-sloped contour segment, consistent with that explanation. The solid line near the filled symbols represents a fit of a two bipolar mechanism model (essentially the $L - M$ and luminance mechanisms of Fig. 1), combined by probability summation.

The right-hand panel of Fig. 5 shows the same no-noise thresholds, but the masked thresholds were obtained in pure M-cone noise (90° in this plane). The M cone noise has qualitatively the same effect as the equiluminant noise; there is no evidence of thresholds being raised more near the noise angle, as there should be if there were multiple mechanisms. The fact that different noises desensitize a mechanism without changing its relative spec-

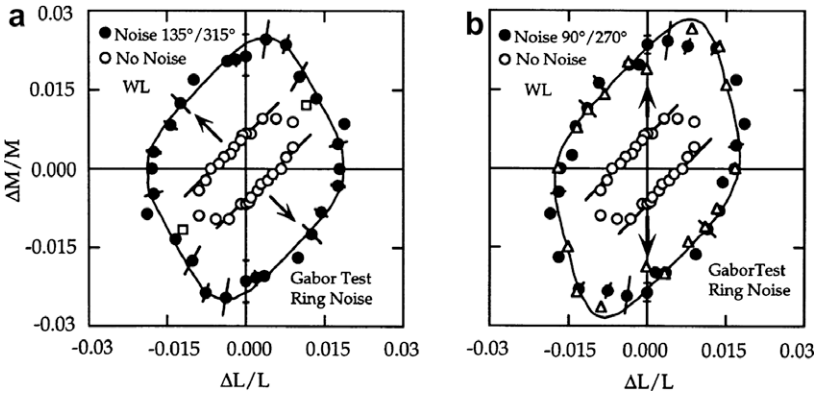

Fig. 5. Detection data from one observer in the (L, M) plane of cone contrast space. The horizontal and vertical axes represent L and M cone contrasts of a 1 cpd Gabor test. The open circles show detection thresholds without masking noise. The filled circles and open triangles show thresholds collected in the presence of masking noises (flickering rings) of two color directions, as indicated by the double-arrows: (a) approximately-equiluminant noise, at 135°/315° in the plane; (b) M cone noise, at 90°/270°. Reprinted Fig. 5 from Vision Research, Vol. 38, Giulianini, F., & Eskew, R. T., Jr., "Chromatic masking in the ($\Delta L/L$, $\Delta M/M$) plane of cone-contrast space reveals only two detection mechanisms", copyright 1998, with permission from Elsevier.

tral sensitivity – the slope of its detection contour in the two panels does not change – is a key test of one of the properties of mechanisms as defined here. The *M* cone noise has the expected greater effect on the putative luminance mechanism (the negatively-sloped contour segments), than did the approximately-equiluminant noise in the left-hand panel. The detection contours are broad, rather than being narrowly elongated along either noise direction. Broad tuning was also shown in substantial field sensitivity data from Sankeralli and Mullen (1997).

A complication is that the negatively-sloped portion of the masked detection contour seems to be steeper in the right-hand panel of Fig. 5; this might suggest a failure of the constant spectral sensitivity assumption. Another possibility discussed in the paper is that the very steep set of thresholds near the *L* cone axis indicates intrusion of an additional mechanism. That need not be a higher-order mechanism, however, as both the luminance and the long-wave portion of a mechanism like $S-(L+M)$ could contribute to these thresholds. An important point to note here is that even the cardinal model predicts that up to three bipolar (Fig. 1a) or six unipolar (Fig. 1b) mechanisms could contribute to detection in this plane, depending on condition, illustrating the difficulty of modeling data of this sort.

Eskew et al. (2001) measured detection contours in the equiluminant plane using 1 cpd Gabor patches and flickering noise lines; sample data are shown in Fig. 6. Again the open symbols are the no-noise thresholds, and the filled symbols show the masked data in the presence of noises of color angle indicated in the upper right of each panel. When the noise is along the *S* cone ($90^\circ/270^\circ$) axis (bottom two panels), tuning appears narrow – only the *S* cone tests are much masked. The narrow detection contour in this case is consistent with linear mechanisms, since these are test (rather than field) sensitivities and the putative mechanisms differ in sensitivity by a large factor. For the other noise angles (including individually-determined equiluminant angles), the broad tuning of masking is like the results of Giulianini and Eskew (1998) and Sankeralli and Mullen (1997), and all the data were modeled as probability summation of cardinal-like mechanisms. However, a clear weakness of this study and the Giulianini and Eskew (1998) one was that noise was never placed in the corner of the detection contours.

In addition to noise, Gegenfurtner and Kiper (1992) used chromatic gratings as masks, and found maximum threshold elevation at the mask chromaticity even for non-cardinal masks. However, Stromeyer, Thabet, Chaparro, and Kronauer (1999) showed that grating masks create a phase offset cue that could produce the alignment of the grating-masked detection contours with the non-cardinal tests. In a recent paper, Hansen and Gegenfurtner (2006) used a stimulus arrangement that should minimize spatial phase offset cues. This study is particularly complete, using a large number of stimulus conditions and a total of seven observers. The stimulus was a checkerboard of 0.5° square elements, each of which could be modulated independently. Noise and test chromaticities were summed within a noise check, and so were spatially-aligned: there was no spatial offset between the test and the noise, and no obvious way to create the phase offset cues identified by Stromeyer et al. (1999).

The test consisted of a 6×1.5 rectangular block of 0.5° squares, flickering at 15 Hz, with chromaticities drawn from a single line in the equiluminant plane, including both color polarities. This test region was oriented either vertically or horizontally, and the observer's task was to discriminate those orientations. The test was embedded in dynamic noise of two types. The first type, "single-sided" noise, had chromaticities drawn from a single chromatic direction (like the test). Detection contours were measured in the equiluminant plane, with six different noises of constant power.

Fig. 7 shows results for one observer. Each panel represents a different test color direction (indicated by the solid line). The threshold-elevating effect of the noise at each test color angle are represented by the difference between the no-noise (gray) and noise conditions. Maximal masking was obtained when noise and test were aligned and minimal (close to zero) masking when they were orthogonal. Very similar results were found in a plane spanned by the $L-M$ and equichromatic ("luminance") axes. There is no evidence that the cardinal axes have any special status in these data.

Hansen and Gegenfurtner (2006) also fixed the noise direction, and varied the test direction (a test sensitivity experiment). As before, when threshold was plotted as a function of the difference between the test and noise angles, the resulting tuning curve was much narrower than a cosine, implying some form of nonlinearity. Following D'Zmura and Knoblauch (1998) and Hansen and Gegenfurtner (2006) attribute this nonlinearity to "off-axis looking", in which the observer's decision is based upon the least masked of a set of mechanisms with overlapping sensitivities; this behavior (whether based upon a conscious strategy or not) would minimize masking when the noise is off the test axis and thereby narrow the tuning curve.

Previously, D'Zmura and Knoblauch (1998) had attempted to eliminate the influence of off-axis looking by using two noise components: one noise vector aligned with the test, and another at right angles to it. The resultant noise is 'sectored – a wedge of noise centered on the test. D'Zmura and Knoblauch varied the length of the orthogonal vector, and thus the width of the sector of noise. If the test is detected by a linear mechanism tuned to the test color direction, this second, orthogonal vector will have no effect, regardless of its length (contrast); the first noise component is always aligned with the test and therefore does not permit off-axis looking to operate. The result was that, at each of the four studied test directions, the added orthogonal noise had no effect at any contrast. Monaci, Menegaz, Susstrunk, and Knoblauch (2004) also added orthogonal noise to vary sector width, for two cardinal and two non-cardinal test directions, and at three axial noise contrasts. A hierarchical statistical analysis found no effect of sector width on detection of a target centered in the sector, regardless of whether the test was cardinal or not. These studies of sectored noise were limited to a handful of test directions, but if there were no mechanism tuned to the test direction then at least a few of these should have been detected by two cardinal mechanisms and thus been masked by the orthogonal noise, and that did not occur.

Since the orthogonal noise component had little effect in the D'Zmura and Knoblauch (1998) and Monaci et al. (2004) experiments, one might wonder whether it was in fact strong enough, in these particular conditions, to provide a fair test. The second sort of noise used by Hansen and Gegenfurtner (2006), which they called "two-sided" noise, may be viewed as a generalization of the two-component noise of D'Zmura and Knoblauch (1998) that effectively addresses this potential concern (see Lindsey & Brown, 2004 for a different approach to this issue). This two-sided noise had samples independently drawn from two chromatic axes, at symmetric angles about the test direction. Like D'Zmura and Knoblauch's noise, this two-sided noise creates a sector or wedge of noise centered on the test direction.[3]

[3] The noises in both studies may be decomposed into a component that is aligned with the test and another that is orthogonal to it. However, the two-sided noise of Hansen and Gegenfurtner (2006) was kept at constant contrast (the two vectors inscribed a circle) whereas in the D'Zmura and Knoblauch (1998) study the equivalent contrast would be $(1/Cos(\theta))$, a line orthogonal to the test vector. In the first case, the projection onto the test direction fell off as $Cos(\theta)$, in the second it was constant.

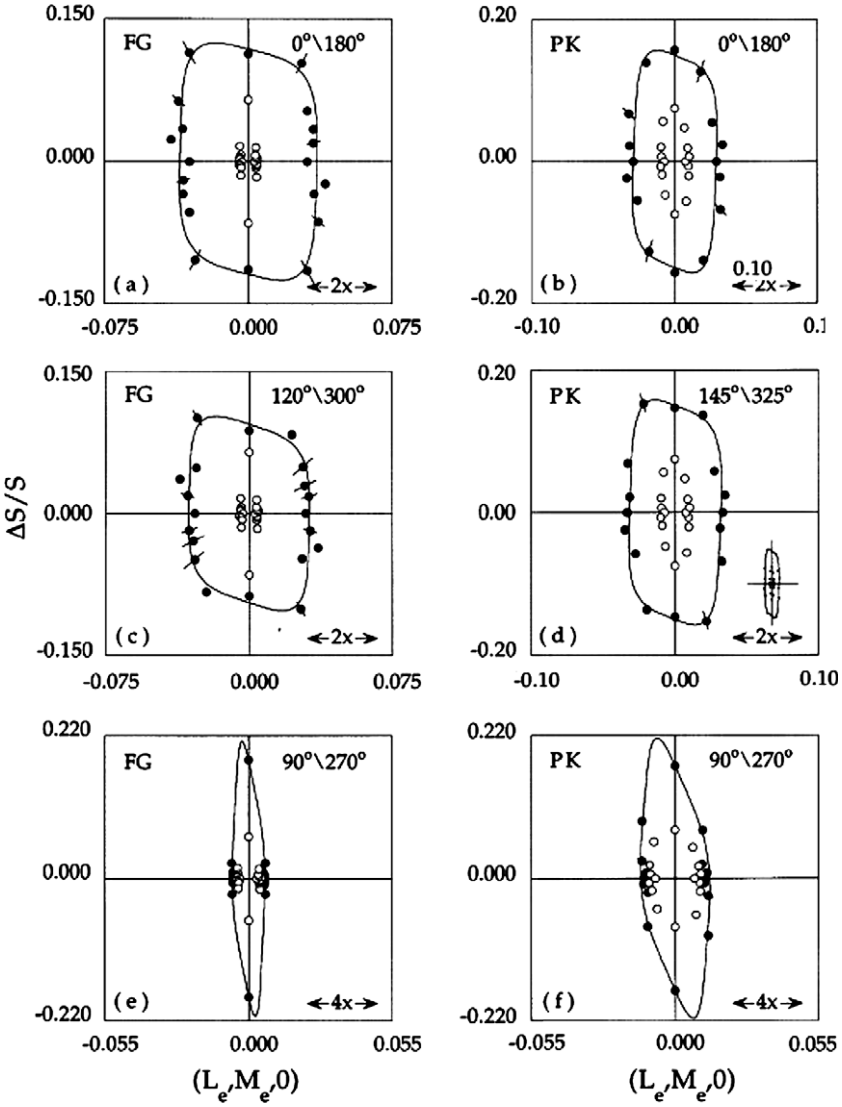

Fig. 6. Detection (test sensitivity) contours in the equiluminant plane for observers FG (left column) and PK (right column). The horizontal axis is the $L - M$ direction (with an individually-determined equiluminant basis vector [L_e, M_e, 0]); the vertical axis is the S cone axis. The open symbols show detection thresholds for 1 cpd Gabor patches; points are plotted twice, for the two symmetric peaks of the stimulus translated across the origin. The filled symbols show detection for the same stimuli embedded in randomly flickering lines. Three noise axes are shown: $L - M$ (0°/180°) in the top panels, S cone noise (90°/270°) in the bottom panels, and an intermediate axis in the middle panels. Note the horizontal axis has been expanded 2X to 4X, as indicated in the bottom right of each panel; the actual aspect ratio one of the contours is shown in the inset to panel (d). Reprinted Fig. 1 from Vision Research, Vol. 41, Eskew, R. T., Jr., Newton, J. R., & Giulianini, F. "Chromatic detection and discrimination analyzed by a Bayesian classifier," pp. 893–909, copyright 2001, with permission from Elsevier.

Assuming the distribution of mechanism preferences is approximately symmetric about the test direction (which must be true if there are a large number of mechanisms), off-axis looking will not distort the tuning curve with the two-sided noise (variation in the threshold for the fixed test as a function of the sector width). For both the equiluminant and $L - M$/equichromatic plane, the masking was broader than with the single-sided noise, and orthogonal noise produced little (not always no) masking; this last condition is identical to the D'Zmura & Knoblauch experiment (at one contrast). Fig. 8 shows data from the equiluminant plane. The tuning curves were approximately cosinusoidal (not shown), but did not now peak at the direction of the test, but rather some 10–30° away – a reflection of the 'bow-tie' pattern seen in many of these field sensitivity curves. The broader curve is expected if there are linear mechanisms, and is consistent with the suggestion that the narrow turning with single-sided noise is due to off-axis looking, but the phase shift is hard to explain if there are many linear mechanisms; for example, even the authors' 16 mechanism model did not produce this shift (their Fig. 14).

Although most of the noise masking results of Sankeralli and Mullen (1997) are consistent with a cardinal-like model, showing cosine tuning of the noise effect and maximal masking at the putative mechanism direction rather than the test direction, one condition seems to be an exception. An L cone test was maximally masked by L cone noise (their Fig. 9), even though this direction is not a mechanism direction for the cardinal mechanism model or any plausible variation of it. Moreover, noise tuning for this L cone test was narrower than a cosine. The authors suggested that this might result from higher-order mechanisms tuned to this intermediate direction, or from the phase cues discussed by Stromeyer et al. (1999) appearing in the spatial frequency components of their broad-band noise stimulus. However, the L cone test does not isolate a single mechanism according to the cardinal model: the L cone test could be detectable to both the $L - M$ and $L + M$ mechanisms, and thus off-axis looking should operate when one of these two mechanisms was desensitized by the noise, accounting for the narrow tuning function. Maximum masking would be obtained with a noise that masked *both* cardinal mechanisms

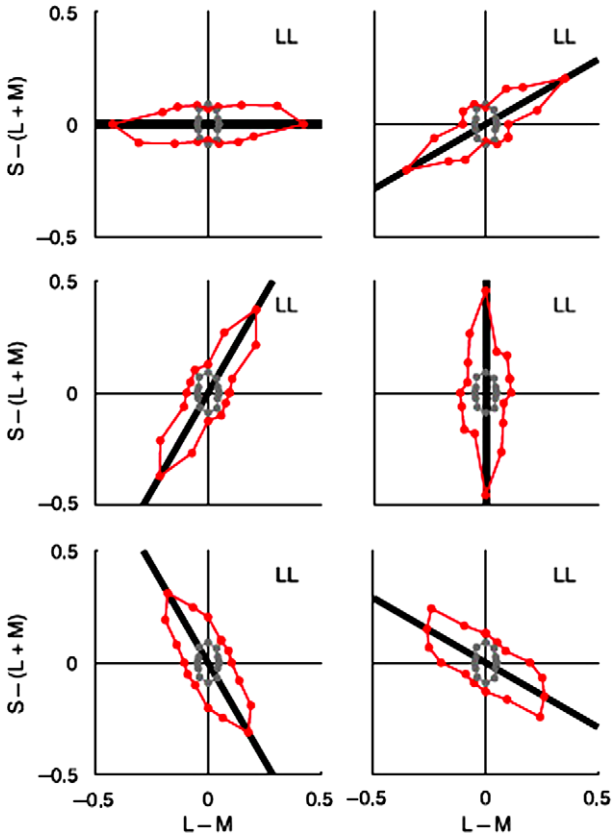

Fig. 7. Field sensitivity contours using "single-sided" noise in the equiluminant plane for one representative observer. The task was to detect the orientation (vertical vs. horizontal) of a large rectangle of flickering color squares. The test color direction is given by the heavy line in each panel. The gray points near the origin indicate the threshold of that test without noise; the deviation of those points from a circle indicates the relative scaling of the two axes. The red points falling on the narrow contour aligned with the test are the thresholds as masked by "axial" noise at the angle of the red point. The two cardinal axes, plus four intermediate ones, were used for the test. Reprinted Fig. 6 from Journal of Vision, Vol. 6, Hansen, T., & Gegenfurtner, K. R. (2006). pp. 239–259, copyright 2006, The Association for Research in Vision and Ophthalmology.

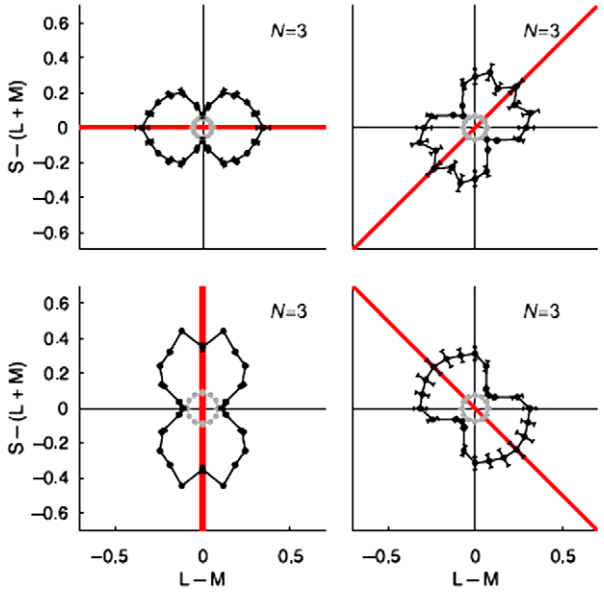

Fig. 8. Masking with "two-sided" noise. Average of three observers. In each panel, the heavy line shows the test color direction in the equiluminant plane. Each point represents masking produced by a pair of noise vectors, symmetrically disposed about the test direction, separated from the test by the angle between the point and the test direction. Reprinted Fig. 15 from Journal of Vision, Vol. 6, Hansen, T., & Gegenfurtner, K. R. (2006). pp. 239–259, copyright 2006, The Association for Research in Vision and Ophthalmology.

approximately equally. Simple mathematics shows that in the plane defined by the $L - M$ and equichromatic ($L + M + S$) axes used by Sankeralli and Mullen, the direction that jointly masks the two mechanisms most is near the projected L cone direction.[4] Thus these results are in fact quite consistent with the cardinal axis model.

The same logic applies to some of the other noise masking studies that used tests at intermediate angles, for example Hansen and Gegenfurtner (2006), their Fig. 10, which is very similar to the example from Sankeralli and Mullen (1997) just discussed. It is not obvious, however, that this explanation could explain the different results in the upper right and middle left panels of the current Fig. 7, in which two intermediate angles, close to one another, each produced maximum masking – unless there are more than two mechanisms active in this plane (as Hansen and Gegenfurtner suggest), or the mechanisms are nonlinear, or both.

[4] If the $L - M$ mechanism is at 0° in the plane, and the $L + M$ mechanism projects into 90° in the plane, joint noise masking of the two could be modeled as $Cos^2(\alpha)Cos^2(\alpha - 90) = Sin^2(2\alpha)/4$, which peaks at $\alpha = 45°$, near the projection of the L cone stimulus (at 39° for unit length basis vectors in this plane).

In summary, a number of studies of noise masking of chromatic detection have been published. Early evidence favoring multiple narrowly-tuned mechanisms (Gegenfurtner & Kiper, 1992) has been re-interpreted as evidence of off-axis looking rather than nonlinearity of cone combination (D'Zmura & Knoblauch, 1998; Hansen & Gegenfurtner, 2006; Lindsey & Brown, 2004; Monaci et al., 2004). However, other noise masking data (Eskew et al., 2001; Giulianini & Eskew, 1998; Newton & Eskew, 2003; Sankeralli & Mullen, 1997) suggests a limited number of mechanisms, and Giulianini and Eskew (2007) provide evidence against off-axis looking affecting S cone tests. All of these latter studies represented data in cone contrast rather than MBDKL space, which may have influenced the choice of color angles used (see Section 12); in particular, since thresholds in cone contrast units differ by a factor of 10 or more across different angles (Cole, Hine, & McIlhagga, 1993; Eskew et al., 1999; Sankeralli & Mullen, 1996), users of cone contrast space might be less likely to select color angles in the corners of the elongated detection contours. However, the patterns of masking do not seem to require that *any* particular angle in MBDKL space be used (D'Zmura & Knoblauch, 1998; Hansen & Gegenfurtner, 2006) – the particular color direction does not seem to be important in the studies finding evidence for higher order mechanisms (in MBDKL space). There is thus no obvious reason that the choice of color representation would make such a consistent difference. Attempts at direct replication of experiments across labs may be necessary to resolve these empirical discrepancies.

11. Chromatic discrimination

This section examines experiments which have measured chromatic discrimination at and near detection threshold. As noted in Section 6, the logic here is different from the auxiliary stimulus manipulations described in the preceding sections. The logic of the chromatic discrimination experiments is based upon the uni-

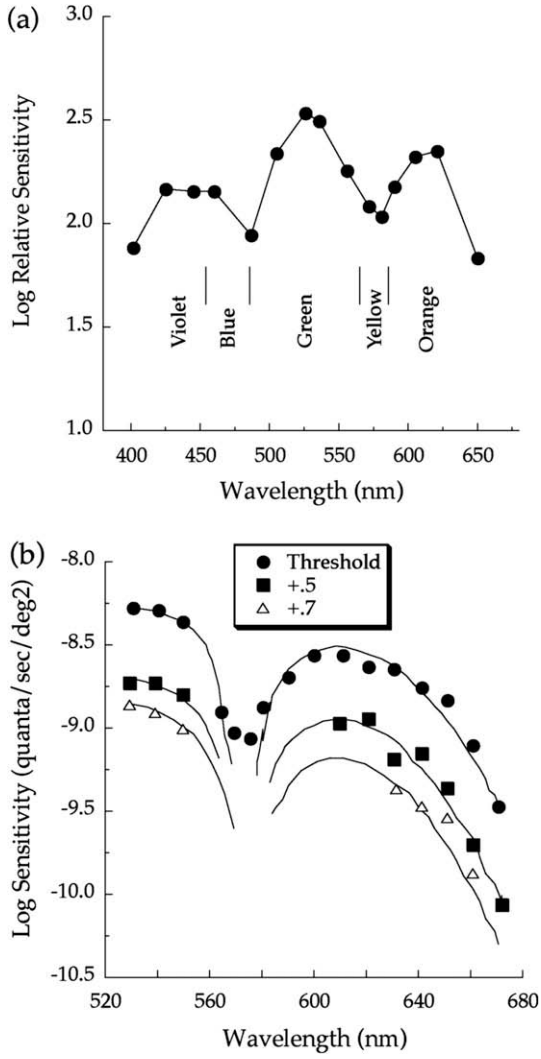

Fig. 9. (a) Relative spectral sensitivity, for observer KTM, for flashes presented against a white background. Pairs of wavelengths within each of the labeled hue bands could not be discriminated, while discriminations across bands (across the vertical lines) were perfect, except for the partial discrimination between the 'violet' and 'blue' regions. From Fig. 9a of (Mullen & Kulikowski, 1990), used with permission. (b) Spectral sensitivity (filled circles), for observer DC, for flashes presented against a 578 nm background (circles). On each side of the Sloan notch at 578 nm, the squares or triangles (0.5 and 0.7 log units above threshold, respectively) are indiscriminable. Reprinted Fig. 7 from Vision Research, Vol. 32, Calkins, D. J., Thornton, J. E., & Pugh, E. N., Jr. "Monochromatism determined at a long-wavelength/middle-wavelength cone-antagonistic locus", pp. 2349–2367, copyright 1992, with permission from Elsevier.

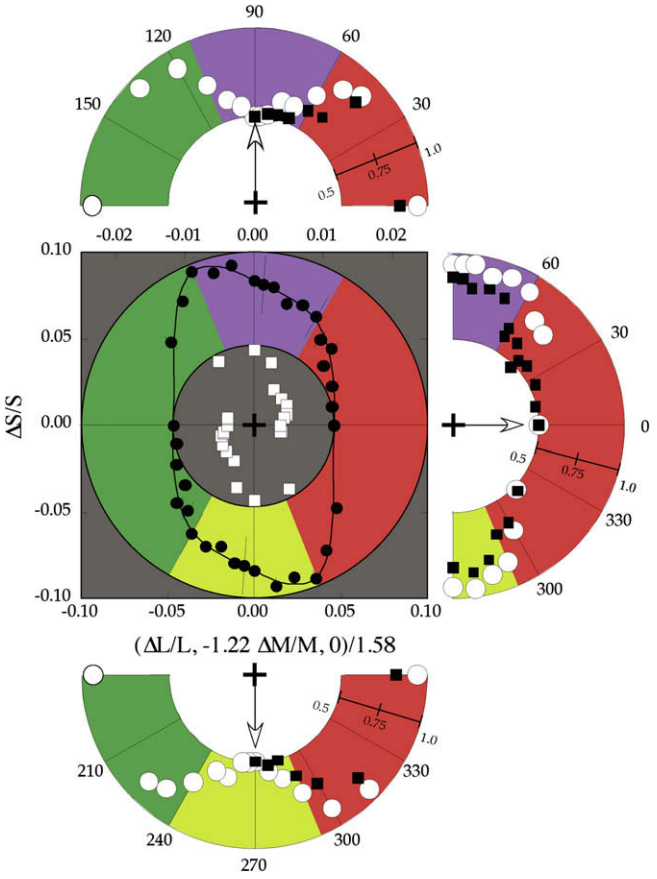

Fig. 10. Detection and discrimination in the equiluminant plane. The center square panel shows detection thresholds for Gabor patches with (filled symbols) or without (open symbols) red/green masking noise (0°/180° color direction). Note that the horizontal scale is expanded for the no-noise thresholds represented by the open symbols, and is represented on the top axis. The weighting constants on the $L - M$ contrast axis result from using unit-length basis vectors in the equiluminant plane. Data are symmetric about the origin due to the symmetric stimuli. The solid black line fitted to the masked thresholds represents probability summation among four symmetric unipolar linear mechanisms. The three arcs are polar plots, with the angular coordinate referring to the same stimuli, at the same angles, as in the detection data. The radial coordinate gives the discriminability (between 0.5 and 1.0) of the given test color angle with the standard color angle indicated by the arrow. Solid symbols are data, open symbols are predictions of a Bayesian classifier model that takes the outputs of the four mechanisms fitted to the detection data as its inputs. All the parameter fitting was done in estimating the detection model; the discrimination predictions are made with no free parameters. Colored regions indicate bands of poorly discriminated stimuli, and are redrawn on the detection plot for comparison. The greenish indiscriminability region was taken from model fit and data from other observers. Reprinted Fig. 5 from The senses: a comprehensive reference (Masland & T. D. Albright (Eds.), Vol. 2: Vision II., pp. 101–117, "Chromatic detection and discrimination," copyright 2008, with permission from Elsevier.

variance and labeled line assumptions (Section 5). Taken together, these two assumptions imply that if and only if two threshold-level stimuli are detected by the same mechanism will the two stimuli be indiscriminable.

Mullen and Kulikowski (1990) presented monochromatic, flashed spots against a white background using a "2 × 2" procedure (Watson & Robson, 1981). Two intervals were presented in a trial, with one of two randomly-chosen wavelengths presented in a randomly-chosen interval. Observers had to identify both the interval and the wavelength. Across runs, wavelengths were varied. The results showed that there were four bands of wavelengths that could not be discriminated from one another at threshold, but there was good discrimination across bands. In addition, there was a fifth band at short wavelengths that was partially-discriminable from longer wavelengths. These bands were labeled 'orange', 'yellow', 'green', 'blue', and 'violet', and their locations along with relative spectral sensitivity curves are shown in Fig. 9a for one observer. The boundaries between spectral bands were fixed – they did not depend upon which particular wavelengths were used in a given experiment, or simply the wavelength difference between the stimuli. The fact that two wavelength regions are given distinct labels, with a fixed boundary between them, fits the usual definition of categorical perception (Harnad, 1987). Mullen and Kulikowski (1990) report that the 'violet' lights, which were imperfectly discriminable from the 'blue' ones, were well-discriminated from the long-wavelength 'oranges', based upon informal experiments.

Calkins, Thornton, and Pugh (1992) restricted attention to longer-wavelength lights, but measured discriminability up to 0.7 log units above threshold, for flashed monochromatic spots presented

against a bright 578 nm background. Relative intensity was varied to find the intensities at which lights could not be discriminated. The resulting "indiscriminability spectra" had the same shape as the spectral sensitivity at threshold (Fig. 9b). Pairs of wavelengths that spanned the Sloan notch (at the field wavelength – Thornton & Pugh, 1983) were perfectly discriminable, but a pair drawn from one side of the notch could not be discriminated at properly-chosen relative intensities. These results, like Mullen and Kulikowski's (1990), present strong evidence that there are a limited number of labeled-line mechanisms, in this case up to five times threshold, and three, and only three, such mechanisms in the long-wavelength part of the spectrum. Presumably these three mechanisms would correspond to the $L-M$, $M-L$, and luminance mechanisms of Fig. 1b (although the long-wave end of the $(L+M)-S$ mechanism might in principle also contribute in the Sloan notch; Newton and Eskew (2003) provide evidence for that intrusion under conditions in which the other mechanisms are less sensitive, in the periphery).

In the original higher-order color mechanism paper, Krauskopf et al. (1986) also studied chromatic discrimination at threshold, and, like Mullen and Kulikowski (1990), used a variation on the 2×2 method. Pairs of chromaticities separated by 90° in the equiluminant plane were used. If there are only cardinal axis mechanisms, and they are labeled lines, the cardinal pairs should be as discriminable as they are detectable (Watson & Robson, 1981), but the non-cardinal pairs (e.g., 45° and 135°) should not: because an intermediate stimulus should be detected sometimes by one cardinal mechanism, sometimes by the other, and sometimes by both, detection should be better than discrimination, as a rule. Almost all the intermediate pair discriminations were better than predicted on this basis, and Kraukopf et al. concluded that this was evidence that the intermediate tests were detected by higher-order, labeled line mechanisms, not by the cardinal ones. However, there are two concerns with this argument: (a) If (for example) the nominally 45° stimulus was not actually equally detectable to two cardinal mechanisms, the quantitative analysis would be in error – and the error would be that discrimination would be better than predicted, as found. (b) The analysis depends upon the high-threshold correction for guessing, known to be wrong in other contexts (Graham, 1989; Laming, 1973).

Eskew et al. (2001) and Newton and Eskew (2003), also combined measurements of detection thresholds with discriminability, and tested a four mechanism, cardinal-like model. In both studies, a fixed masking noise was present (for both detection and discrimination), in order to desensitize the highly-sensitive $L-M$ and $M-L$ mechanisms and and attempt to reveal higher-order mechanisms. Eskew et al. (2001) used 1 cpd Gabor patches, presented to the fovea. Some of the data are shown in Fig. 10. The central panel shows detection data. The open symbols show no-noise thresholds (with the horizontal axis expanded, and given at the top). The filled symbols show thresholds in the presence of noise lines, flickering randomly between red and green (0° and 180°, the horizontal axis of the plot). As in Sankeralli and Mullen (1997) and Giulianini and Eskew (1998) (Fig. 5), the masking effect of the noise was generally broad, disagreeing with Gegenfurtner and Kiper (1992) and Hansen and Gegenfurtner (2006). The solid line represents a model based upon four half-wave linear mechanisms (Fig. 1b) combined by probability summation.

These authors used a discrimination procedure to test this cardinal-like model. Pairs of threshold-level stimuli (in the presence of the noise), were presented in random order to the observer, who had to pick the designated "standard" color pairs (because these were Gabor patches, the discrimination was of a color at a particular spatial phase). The three arcs in Fig. 10 represent discrimination data (filled symbols) and model predictions (open circles) in polar coordinates. Within each arc, the angular coordinate represents the angle of the stimulus (same angles as in the central panel of detection data), and the radial coordinate represents the proportion of tests that were discriminable from the standard. Three standards are shown (arrows). Consider the right-hand arc, with a standard stimulus represented along the 0°/180°, red–green horizontal axis. The observer was unable to discriminate this standard from tests lying between about 290° and 60°; these angles have been colored red. In contrast, tests lying above 60° (purple) or below 290° (yellow) were readily discriminable from the standard. Taken together with other data not shown here, the results of this experiment suggest only four spectral bands of indiscriminable stimuli in the equiluminant plane.

The filled squares show the prediction of a Bayesian classifier model, which takes the output of the four mechanisms and makes an optimal discrimination decision. The parameter fitting was done entirely in fitting the detection model; the classifier prediction was made, for all of the standard colors together, with no free parameters. The inefficient human (open circles) generally performed worse than the optimal classifier (filled squares) in the critical transition regions, which is unsurprising.

Fig. 11 shows results from an analogous experiment conducted in the (L, M) plane, with 2° test spots presented 18° in the periphery (Newton & Eskew, 2003). Detection thresholds, collected in the presence of achromatic masking noise, are indicated by the filled circles; a post-receptoral difference in sensitivity to 'green' is reflected in the slightly greater distance from the origin to the upper, as compared to the lower, long contour segment. As in Fig. 10, the three arcs represent discrimination of threshold-level tests from three different standards (arrows). The model predicts that the standards at 113° (upper left) and 293° (lower right) were detected by $M-L$ and $L-M$ (G and R, see below) mechanisms, respectively, and the discrimination data show that the thresholds that fall

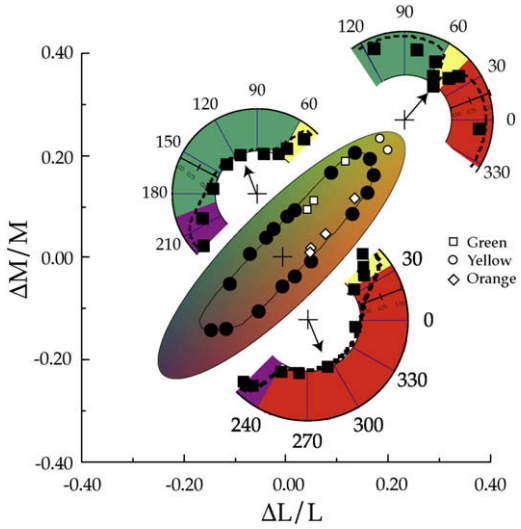

Fig. 11. Detection and discrimination in the (L, M) plane, like Fig. 10, but for 2° test spots presented at 18° eccentricity. The central elliptical region represents a detection contour in the (L, M) plane of cone contrast space, measured in the presence of masking noise along the (45°/225°) direction (the no-noise detection contour is not shown here, but it is clearly nonelliptical). The three arcs are polar plots, with the angular coordinate referring to the same stimuli, at the same angles, as the detection data. The radial coordinate within each arc gives the discriminability (between 0.5 and 1.0) between the given test color angle and the standard color angle indicated by the arrow, as in Fig. 10. In this figure the dashed line gives the Bayesian Classifier model prediction, which was again made without free parameters. Adapted, with permission, from Fig. 6 of Newton and Eskew (2003). The open symbols show the long-wave thresholds from Fig. 9a, converted into cone contrast units with a single sensitivity scaling factor, with squares, circles and diamonds indicating the appearance of the tests as green, yellow, and orange, respectively.

along the two flanking contours could not be discriminated from those standards (not shown here is the fact that stimuli on the opposite side of the contour from each standard could be perfectly discriminated from that standard). The Bayesian classifier provides a very good account of the discrimination performance, again without use of any free parameters.

In both of these studies (Eskew et al., 2001; Newton & Eskew, 2003), the detection model that formed the basis for the analysis of the discrimination data suffers from making the high-threshold assumption, one criticism of Krauskopf et al. (1986). However, because a wide range of stimulus angles to be discriminated were paired with each standard (within each of the arcs in Figs. 10 and 11), there is no concern that a particular pair of stimuli were exactly equally detectable to two mechanisms as in the Krauskopf et al. study.

The open symbols in Fig. 11 show the longer-wavelength (>525 nm) portion of the foveal spectral sensitivity data of Mullen and Kulikowski (1990), from Fig. 9a, transformed to cone contrasts (see (Eskew et al., 1999) for another example of this type of analysis). Because these are incremental stimuli, and are of long enough wavelength that the S cones do not contribute, the cone contrasts all fall in the first quadrant of the (L, M) plane. The set of thresholds has been scaled with a single factor to match the overall sensitivity of the foveal measurements of Mullen and Kulikowski (1990) with the peripheral measurements of Newton and Eskew (2003). The shape of the symbols indicates the hue band. Even with the differences in observer, equipment, method, and retinal location, the agreement is excellent.

Taken together, these detection/discrimination results suggest that there are a limited number – four or five – of labeled line chromatic mechanisms active at and near threshold. There is some uncertainty about how many mechanisms are contributing in the Sloan notch (the 'yellow' band in Fig. 9 and the narrow end of the contour in Fig. 11); both theory and some results suggest at least two ((Newton & Eskew, 2003), a 'yellow' and an increment achromatic mechanism, with these non-equiluminant stimuli. The corresponding decrement band has been even less explored. Further experiments measuring chromatic discrimination at threshold, taken in conjunction with detection data as summarized above, are crucial to deciding between a limited number of possibly complex mechanisms (see Section 13), or a larger number of relatively simple (linear) mechanisms – or doing away with the labeled-line aspect of the definition of mechanism altogether.

12. Conflicting results

There are puzzling empirical disagreements, particularly in the studies of noise masking to which several different laboratories have contributed. Some studies have found no evidence for higher order mechanisms, using noise (and pattern) masks (Giulianini & Eskew, 1998), (Eskew et al., 2001; Newton & Eskew, 2003; Sankeralli & Mullen, 1997; Stromeyer et al., 1999). Others have found such evidence (D'Zmura & Knoblauch, 1998; Gegenfurtner & Kiper, 1992; Hansen & Gegenfurtner, 2006; Lindsey & Brown, 2004; Monaci et al., 2004). Some early experiments found that cardinal axes have a special status (Flanagan et al., 1990; Krauskopf, 1999), but the large majority of papers argue there is nothing different about the cardinal axes in terms of the experimental manipulations used (Clifford et al., 2003; Hansen & Gegenfurtner, 2006; Webster, Malkoc, Bilson, & Webster, 2002), with the possible exception of the luminance axis, which has been less-frequently studied (Gegenfurtner & Kiper, 1992; Krauskopf et al., 1996). In contrast, noise masking results of Sankeralli and Mullen (1997) and Giulianini and Eskew (1998), found only cardinal-like mechanisms.

Where evidence favoring higher order mechanisms has been found, the estimated bandwidth of the effect of the auxiliary stimulus, and implied linearity of the underlying mechanisms, have varied greatly. Narrow tuning of noise masking (Gegenfurtner & Kiper, 1992; Hansen & Gegenfurtner, 2006) has been attributed to off-axis looking (D'Zmura & Knoblauch, 1998; Lindsey & Brown, 2004; Monaci et al., 2004); since off-axis looking is an optimal strategy in these detection tasks if there are enough mechanisms to support it for a particular condition (MacLeod, cited in D'Zmura & Knoblauch, 1998), the broad tuning found by other researchers (Eskew et al., 2001; Sankeralli & Mullen, 1997) reflects either suboptimal performance by their observers or is indeed evidence that there are a limited number of mechanisms.

When noise or other adapting stimuli are used as auxiliary (field) stimuli to measure tuning functions, the strength of the stimulus (noise power) must be kept constant to obtain interpretable results. This means that in a given plane of color space, the color direction where the instrumental gamut is weakest determines the maximum stimulus strength at all color angles, raising a possible concern with small-signal linearity. Giulianini and Eskew (2007) developed a novel technique, called noise superposition, which permits the use of maximum contrast stimuli at all color angles and therefore does not suffer from this potential small-signal linearity problem. With this technique, strong evidence for nonlinear cone combinations in the detection of S-cone increment and decrement stimuli was found, and there was evidence against off-axis looking. Sankeralli and Mullen (1997) found that noise masking of S cone tests was somewhat more narrowly tuned than a cosine (their Fig. 8), consistent with a deviation from linearity in the combination of cone signals for mechanisms detecting an S cone test (or, in this case, off-axis looking).

With tasks other than noise masking, tuning of the effect of the auxiliary stimulus has been reported to be broad in some experiments (Cardinal & Kiper, 2003; Flanagan et al., 1990; Webster & Mollon, 1994) and narrow in others (Clifford et al., 2003; Goda & Fujii, 2001; Wilson & Switkes, 2005). In their positional adaptation study, McGraw et al. (2004) found broad bandwidths for stimuli near the $L-M$ axis and narrow ones close to the S cone axis (for higher contrast patterns – McKeefry et al., 2004), consistent with the other evidence for nonlinearity in S cone mechanisms (Giulianini & Eskew, 2007; McLellan, & Eskew, 2000; Pugh & Mollon, 1979; Zaidi, Shapiro, & Hood, 1992). It is not clear, in these non-detection tasks, whether some analog of off-axis looking should play a role; if not, one must interpret narrow tuning as indicating intrinsic mechanism nonlinearity in these tasks.

It is possible that some of these discrepancies are due to individual differences. Krauskopf et al. (1986) pointed to some individual differences in the first higher order paper, as did Webster and Mollon later (1994). However, it seems unlikely that this could explain all these differences. Hansen and Gegenfurtner (2006) used a total of seven observers and report no substantial individual differences.

There are some fairly consistent, mundane differences between the experiments finding evidence for higher order mechanisms and those that do not. One is that almost all of the experiments finding higher order mechanisms used binocular viewing (e.g., Gegenfurtner & Kiper, 1992; Goda & Fujii, 2001; Hansen & Gegenfurtner, 2006) – Webster and Mollon (1994, 95027763) is an exception – those not finding higher order mechanisms used monocular viewing (Eskew et al., 2001; Giulianini & Eskew, 1998; Sankeralli & Mullen, 1997). Exclusively binocular chromatic mechanisms, as have recently been claimed to exist (Shimono, Shioiri, & Yaguchi, 2009), might conceivably contribute to higher-order behavior.

Many studies reporting evidence for higher-order mechanisms have used large stimuli (e.g., Cardinal & Kiper, 2003; Clifford et al., 2003; Flanagan et al., 1990; Hansen & Gegenfurtner, 2006;

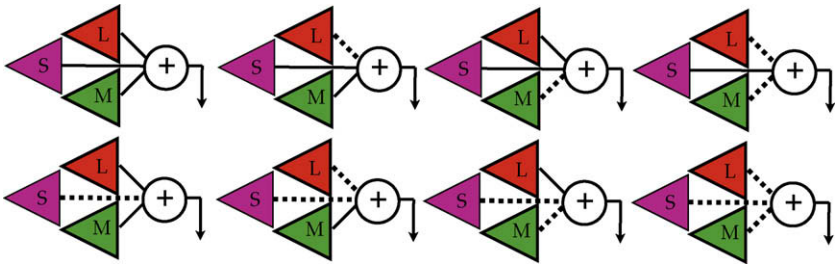

Fig. 12. Eight linear mechanisms, half of the mechanisms in the model of Hansen and Gegenfurtner (2006). All possible combinations of positive and negative signs of cone signals (solid and dashed lines) are included here. Magnitudes of weights are not shown. The other eight mechanisms of Hansen and Gegenfurtner (2006) would be formed by repeating all of the depicted mechanisms with weights of different magnitudes.

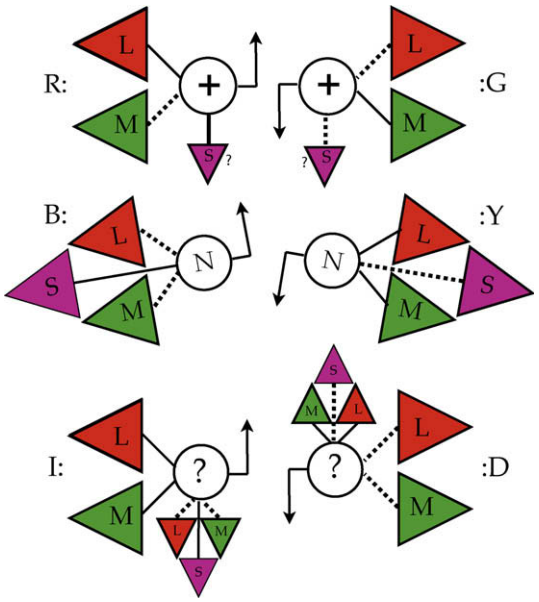

Fig. 13. A model with six mechanisms. *R* and *G* are similar to the $L - M$ and $M - L$ mechanisms of Fig. 1b, but a possible *S* cone input is shown. *B* and *Y* are nonlinear combinations of cone inputs, are asymmetric, and therefore have directions of maximal responsivity that are not complementary in cone space. *I* and *D* ('increment' and 'decrement') are also potentially nonlinear.

Krauskopf et al., 1996; Wilson & Switkes, 2005), perhaps rasing questions about retinal inhomgeneity or luminance artifacts causing stimuli to affect different cardinal mechanisms at different retinal loci. However, other studies have used more compact stimuli and still report evidence of higher-order mechanisms (Krauskopf, 1999; Webster & Mollon, 1991, 1994).

A recurring issue has to do with which color space is used, as noted in the discussion of noise masking. Although Sankeralli and Mullen (2001) argued that the color direction that leaves a linear mechanism unstimulated is not necessarily 90° away (orthogonal) from its mechanism direction, depending on how the representation is (linearly) transformed, Knoblauch and D'Zmura (2001) demonstrated that this claim is incorrect. As Knoblauch and D'Zmura note, if a stimulus is found that does not produce a response in a linear mechanism, that stimulus will not produce a response regardless of which color space the experimenter chooses to use to represent the stimulus.[5]

[5] The present author has noted that the *apparent* shape of a tuning curve can be altered by transformations between color spaces (Eskew & Giulianini, 2005); this is not true, however, if the researcher keeps noise powers and angles constant in the same space in which the data are analyzed, as Hansen and Gegenfurtner (2006) were at pains to do

But it cannot be just a coincidence that all the studies finding evidence for higher order color mechanisms have represented their data in MBDKL space, and the studies failing to find such evidence have used cone contrast space (or wavelength representations), even though the two cone spaces are linearly related as long as the adaptation state is held constant (Eskew et al., 1999). As mentioned above, the choice of color spaces undoubtedly influences the experimenter in choosing stimuli for the experiment (Stockman & Brainard, in press): someone working in cone contrast space is likely to pick a different set of stimuli than someone working in MBDKL space. However, as noted previously, there is no specific reason to believe that the choice of tested angles has produced these differences, as the studies finding evidence for higher order mechanisms have generally also found no special status for any particular color angle.

The linear algebraic argument made by Knoblauch and D'Zmura (2001) does not take experimental error into account as it influences the interpretation of results. Suppose a null stimulus is found that is "close" to the predicted null direction in one color space – when transformed to a new space, that stimulus may not seem close at all. Future researchers on this topic might find it useful to use both color representations in parallel, or at least report thresholds in units (such as cone contrasts) that would permit a comparison of absolute sensitivity across studies. It would help to know whether a higher-order result consisted of thresholds that are lower or higher than a non-higher-order result. If cardinal-like results are associated with lower thresholds it would suggest that higher order mechanisms are less sensitive than cardinal ones, for example, and that might help explain differences across studies. Reporting data only in threshold-normalized coordinates eliminates the information that would allow such comparisons.

The ability – and just as important, the inability – of observers to discriminate the colors of the appropriate liminal stimuli is consistent with a limited number of classical mechanisms and categorical hue perception (Calkins et al., 1992; Eskew et al., 2001; Mullen & Kulikowski, 1990; Newton & Eskew, 2003) The limited data of Krauskopf et al. (1986) is the sole exception known to this author. It could be that higher-order mechanisms are not univariant, labeled lines (Eskew et al., 2001), although they were certainly conceived of that way by Krauskopf et al. (1986). However, from a computational perspective it would not make much sense for higher order mechanisms to be unlabelled; there would seem to be little reason for their existence unless they signal color.

A related point has to do with the difference between linear, broadly-tuned higher-order mechanisms, and nonlinear, narrowly-tuned ones. Narrowly-tuned mechanisms could represent specific hues. Thus narrowly-tuned higher order mechanisms could provide a read-out of lower level color mechanisms for use in representing object color. Broadly-tuned linear higher-order mechanisms would not serve this function; another layer of machinery would be required to compare their outputs in order

to code for specific hues, just as some comparison (such as taking ratios between mechanism outputs – Sankeralli, Mullen, & Hine, 2002) would be required to code for specific hues from cardinal mechanisms. In other words, a broadly-tuned set of multiple chromatic mechanisms would be an intermediate-level representation, not a truly high-level one, whereas narrowly-tuned mechanisms might be thought of as actually high level.

13. Models

Evidence summarized above clearly shows that the cardinal axis model (Fig. 1a or b) is incorrect. The only question is what kind of mechanisms, and how many, are to replace the cardinal ones. Is a limited number of more complex mechanisms, or a larger number of simple mechanisms, better able to account for the data?

Only a handful of studies have explicitly tried to estimate the number of higher-order mechanisms. Webster and Mollon (1994) used broad distributions of mechanisms around the cardinal axes, rather than having discrete channels; their color matching data required substantial variability in chromatic tuning. In the equiluminant plane, Zaidi and Halevy's (1993) model of dynamic chromatic discrimination required more than four mechanisms, and Goda and Fujii's (2001) texture discrimination model required 5 or 7 depending on observer. Hansen and Gegenfurtner (2006) applied models with 4, 8, and 16 linear mechanisms and found that 4 mechanisms could not account for their results, and 16 provided a better fit than 8. Fig. 12 shows eight linear mechanisms, half of those in the best-fitting Hansen and Gegenfurtner (2006) model. To fit this model to a set of data by estimating its cone weights (which Hansen and Gegenfurtner did not do) would require determining 48 free parameters. It is difficult to see how a model with so many mechanisms could account for masking data such as those in Figs. 5 and 6, or the data of Sankeralli and Mullen (1997), to say nothing of the chromatic discrimination data in Figs. 10 and 11 – unless these are not labeled lines.

Rather than having a relatively large number of mechanisms with fixed spectral sensitivities, some models assume that mechanisms interact in such a way as to alter color tuning. As mentioned previously, Atick et al. (1993) showed that an 'adaptive decorrelation' algorithm could alter the gains in post-receptoral mechanisms, following habituation, and account for the asymmetric color matching of Webster and Mollon (1991), essentially rotating the pattern of matches as in Fig. 2. Adaptive processes like this violate one of the assumptions in the definition of color mechanism given earlier, because the relative spectral sensitivity of a mechanism would change (and not as the result of cone-specific adaptation). Adaptive re-weighting of cone signals might account for habituation, and perhaps the results on positional adaptation (McGraw et al., 2004). Noise masking could produce contrast adaptation, and perhaps an adaptive re-weighting could account for some of data such as in Fig. 7; but why then is no rotation of the

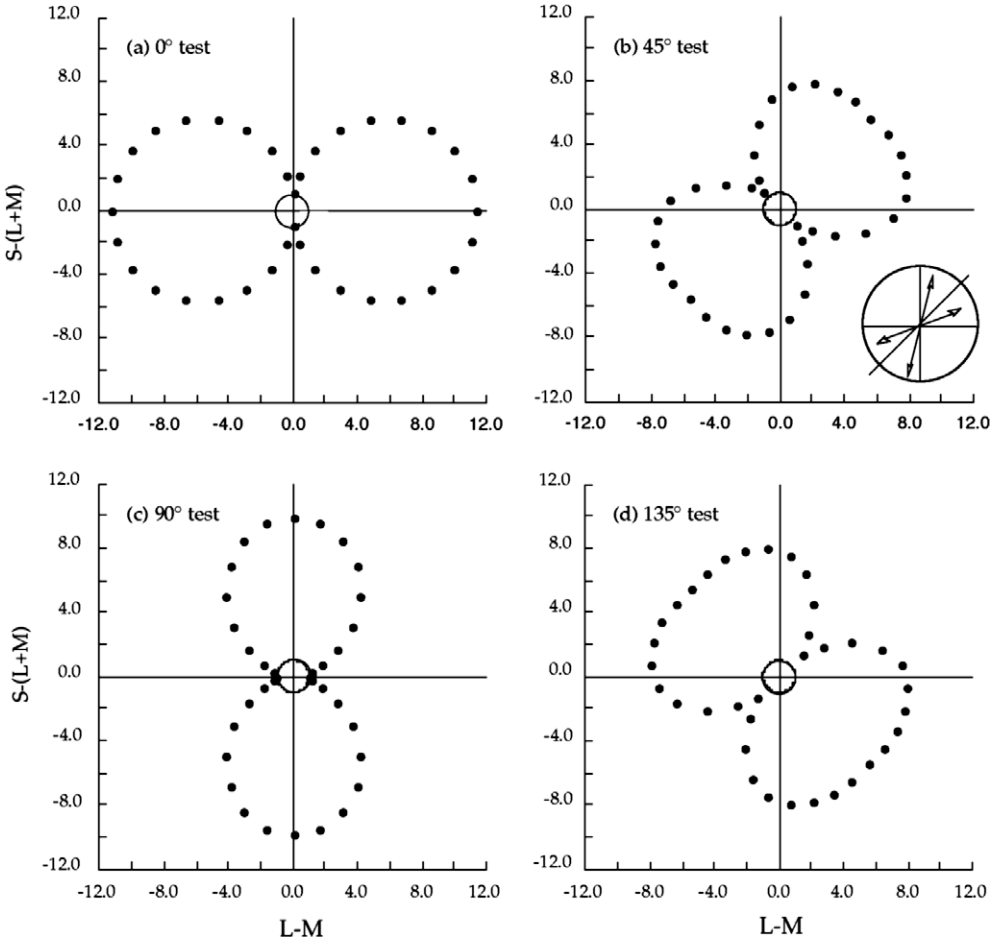

Fig. 14. Simulation of the "two-sided" noise experiment of Hansen and Gegenfurtner (2006), as shown in Fig. 8. Four different test directions are shown. The model had four mechanisms, combined by probability summation (Minkowski exponent of 4.0). Two mechanisms were the linear *R* and *G* of Fig. 13 (with no *S* cone input, so tuned to 0° and 180°). The other two mechanisms were *B* (tuned to 70°) and *Y* (tuned to 285°), with a symmetric nonlinearity modeled by raising a cosine to the third power. The four mechanisms had equal sensitivity. Units on the axes are arbitrary.

contour seen in Figs. 5 and 6, or Fig. 11? Unless some subtle difference in stimulus conditions can be identified that explains the empirical discrepancy, adaptive decorrelation could not account for all the noise masking results.

Stockman and Brainard (in press) demonstrate that if experimental conditions change the site of the noise that limits performance in a detection task – from, say, the receptor to the post-receptoral mechanism – the orientation of a detection contour, and the implied tuning of the mechanism, can change. One way to produce such a change is a saturating nonlinearity, which compresses the input signal and noise and thereby relatively magnifies noise added after the nonlinearity. This kind of process might account for results with transient adaptation, as for example in Krauskopf et al. (1986), where transient shifts in the background could move the system operating point onto flat portions of a nonlinearity (Pugh & Mollon, 1979), and thereby increasing the relative effect of late noise in the system. By the same argument, injecting noise into the system, as in a noise masking experiment, might be expected to de-emphasize late noise sources by making the early, added noise the limiting factor. The expectation might be that noise masking would produce cardinal-like mechanisms – as found in several experiments, but not in others.

Is there a model with few mechanisms that might account for some of the effects that have been attributed to multiple, higher-order mechanisms? The class of potential models to test is very large, especially if nonlinearities of cone combination are permitted. One model, which may be viewed as an extension of the cardinal axis model of Fig. 1b, is shown in Fig. 13. This model has six rectified mechanisms, denoted in the figure as R, G, B, Y, I and D; the last two letters stand for 'increment' and 'decrement', while the others are mnemonics for hues that are similar to those they signal (red, green, blue, and yellow), though they are clearly not hue mechanisms (Krauskopf et al., 1982; Stockman & Brainard, in press; Wuerger, Atkinson, & Cropper, 2005).

Two of the mechanisms, R and G, are very similar to the two poles of the $L-M$ cardinal mechanism, with one exception: a potential S cone input to R or G or both as shown. This input is not consistent with the original cardinal axis study or some other experiments, all of which used field sensitivity methods (Mollon & Cavonius, 1987; Stromeyer & Lee, 1988). However, there is other evidence, collected using test methods, that one or both of these mechanisms receive a very small S cone input (Boynton, Nagy, & Olson, 1983; Eskew & Kortick, 1994; Stromeyer et al., 1998). It could be that there are versions of these mechanisms both with and without S cone inputs. The idea is that when S cone inputs to R and G are measured directly using test methods, they are found, but when habituation or other field methods (with an S cone auxiliary stimulus) are used, the R and G mechanisms with S cone inputs are desensitized and those without the S input take over, a version of off-axis looking. This would imply extra R and G mechanisms (call them R' and G') with very similar spectral tuning to R and G, since the S cone weight is small at best. This S cone input, even though it is small in cone contrast units, might account for some of the phenomena attributed to higher-order mechanisms above; in particular, it means that the R' and G' mechanism directions are not at right angles to the S cone axis in the equiluminant plane. In ongoing work from my lab (Eskew, Wang, & Richters, 2003), we have found some evidence for a separate labeled-line "purplish" mechanism that is consistent with this idea, and possibly with the partial discriminability of short wavelengths found by Mullen and Kulikowski (1990). This is potential evidence of a higher-order mechanism based upon an experiment designed for cone contrast space, an exception to the general rule.

The strongest evidence is for two symmetric, linear, highly sensitive mechanisms (R and G in Fig. 13 or $L-M$ and $M-L$ in Fig. 1b), that detect most stimuli at most angles in cone contrast space. R and G appear to be remarkably linear even when the use of noise (Giulianini & Eskew, 1998; Stromeyer et al., 1999) chromatic adaptation (Chaparro, Stromeyer, Chen, & Kronauer, 1995), or tiny (Chaparro, Stromeyer, Kronauer, & Eskew, 1994) or very brief (Eskew, Stromeyer, & Kronauer, 1994) test spots raises thresholds substantially. Giulianini and Eskew (2007) demonstrated linearity in G even when noise raised threshold by as much as 20-fold.

The B and Y mechanisms are shown as having nonlinear cone combinations (the "*N*" in Fig. 13). The nonlinearity would not necessarily be revealed at threshold, due to small-signal linearity (Giulianini & Eskew, 2007), but may be shown by field experiments that raise thresholds substantially. One piece of evidence for that nonlinearity is the shape of the action spectrum of transient tritanopia (McLellan & Eskew, 2000; Polden & Mollon, 1980). The noise superposition method (Giulianini & Eskew, 2007) has provided strong evidence for nonlinear cone combination in S cone detection.

Note that the nonlinearity in B and Y is at the cone combination stage, not at the output (although a saturating nonlinearity at the output would be a plausible addition). An output nonlinearity would have relatively little effect on many tasks, but nonlinearities in cone combination would alter the shapes of detection contours as well as masking tuning functions.

In Fig. 13, the B and Y mechanisms are tilted, to illustrate that they are asymmetric in cone space: the color directions of their maximal sensitivities are not complementary. Evidence for the asymmetry includes transient tritanopia (McLellan & Eskew, 2000) and sawtooth habituation (Shinomori, Spillmann, & Werner, 1999). This asymmetry means that bipolar auxiliary stimuli, such as noise or habituating flicker, will in general have different effects on two different mechanisms at each auxiliary angle. In some cases, these two effects of a single field stimulus would make it appear there are additional mechanisms.

The I and D mechanisms roughly correspond to the two poles of the luminance cardinal mechanism. The evidence regarding linearity of cone combination in I and D is ambiguous (Eskew, 2008), and therefore a "?" is shown in the picture at the combination site. There is, however, very strong evidence that one or both of these mechanisms get a cone-opponent, $L-M$ input, and an S input of inverted sign (Lindsey, Pokorny, & Smith, 1986; Stockman & Plummer, 2005; Stockman, Plummer, & Montag, 2005; Stromeyer, Chaparro, Tolias, & Kronauer, 1997; Swanson, Ueno, Smith, & Pokorny, 1987).

Parts of this model are speculative, but many of its features have substantial experimental support (summarized in Eskew, 2008). It is offered here to make a few concrete points about alternatives to models with many half-wave linear mechanisms such as in Fig. 12. First, note the nonlinear and asymmetric aspects of these mechanisms mean that, in general, no chromatic axis can completely isolate one of them; a high-contrast flickering noise or habituating stimulus will in general always modulate several mechanisms. The potential nonlinearities and asymmetries in I and D mean that they are not silent in any plane; equiluminance does not necessarily eliminate them.

To illustrate that a model of this kind might be able to account for some of the data from higher-order color experiments, the following simulation of the 'two-sided' noise masking experiment of Hansen and Gegenfurtner (2006) was done. Four mechanisms (R, G, B, and Y) were used, with R and G being linear (cosine tuning), and B and Y being modeled as a cosine raised to the third power. R and G were maximally sensitive at 0° and 180° in the equiluminant plane (no S cone input, in other words), and B and Y were asymmetric at 70° and 285°. Combination of outputs was by standard probability summation, with a Minkowski exponent of 4.0 (Eskew et al., 1999). Simulared thresholds are shown in Fig. 14, for tests at two cardinal and two intermediate test axes. At all four test angles, the pattern is similar to the data of Hansen and Gegen-

furtner (2006), as shown in Fig. 8, including the bow-tie like pattern with a small reduction in masking at the test angle, for the intermediate (but not the cardinal) axes.

This model is intended to illustrate that relatively simple changes to the mechanisms of the cardinal model can, in principle, account for some apparently higher-order color phenomena, including having maximum masking near the test and minimum masking 90° away, for all four of these test angles. However, this is not a complete model of the Hansen and Gegenfurtner results; this four-mechanism model does not do a good job accounting for the results with single-sided noise (e.g., Fig. 7 above); it produces narrow lobes aligned with or near the test as was found, but also two smaller lobes approximately at right angles to the test at most test angles. A hint of something like those lobes is seen in the two upper right-hand panels of Fig. 7, but in general this model does not do a good job with any of the studies that have used "single-sided" noises, whether the tuning is narrow (Gegenfurtner & Kiper, 1992; Hansen & Gegenfurtner, 2005) or broad (Eskew et al., 2001; Giulianini & Eskew, 1998; Newton & Eskew, 2003; Sankeralli & Mullen, 1997). Fig. 14 is, however, an existence proof, demonstrating that, at least for some conditions, it is possible for a model with a limited number of nonlinear mechanisms to produce behavior that has been attributed to having many linear mechanisms. Models of this type might account for "higher-order" phenomena, but – assuming the mechanisms are univariant, labeled lines (Eskew, 2008) – their limited number could still be consistent with the obtained fixed, categorical hue boundaries. However, modeling alone is unlikely to explain the differences between results like those in Figs. 6 and 7 unless some key methodological difference(s) can be discovered.

14. Fundamental questions about mechanisms

The empirical discrepancies in the noise masking data summarized above will presumably be reconciled sooner or later. Once there is better agreement on the major findings, modeling will become more useful – and more important.

What form should those models take? What are the properties of the model elements – the mechanisms – that are combined (and how are they combined, a question not addressed here)? Are the mechanisms univariant, labeled-line combinations of cone signals? If so, how can a large number of mechanisms be consistent with the results of threshold-level chromatic discrimination studies? If mechanisms are not univariant, labeled lines, then what role can they play in color vision? How could hue mechanisms be built from non-labeled outputs?

Do the mechanisms have fixed or adjustable spectral sensitivities? If they are adaptable, how can they account for the masking results showing fixed tuning in the presence of noise (e.g., Fig. 5)? How are adaptable mechanisms consistent with fixed color boundaries?

Are there a limited set of high sensitivity mechanisms, more cardinal-like, and a larger set of lower sensitivity, higher-order mechanisms? If so, why do so many studies find no special status of the cardinal directions?

Are mechanisms narrowly or broadly tuned? If there broadly-tuned circuits, satisfying some explicit definition of mechanism, what higher-level circuits might compare the lower-level outputs to represent object colors, and do those circuits satisfy the same definition of mechanism or should they be called something else?

15. Conclusions

In many other sensory domains there are large numbers of mechanisms or channels. Well-known examples include hearing, in which overlapping and multiple critical bands (Fletcher, 1940; Gulick, Gescheider, & Frisina, 1989) populate the frequency range, and spatial vision, in which a great many spatial frequency and orientation-tuned channels (Graham, 1989) apparently operate.[6] Zaidi (2001) has argued that having a multiplicity of mechanisms in spatial vision allows for "fast and reliable" computation, and, by extension, would be useful in color too. However, in color vision, there are only three types of cone photoreceptors in a patch of retina, unlike the many thousands of hair cells arrayed along the basilar membrane (Gulick et al., 1989), or the even the many thousands of spatial samples taken by those same photoreceptors. Thus, although the computational argument may be plausible, the analogy from spatial vision (or hearing) to color vision is problematic: the front ends are very different.

There are also difficulties in drawing analogies from the behavior of cortical cells. The cortical neurons that have been studied electrophysiologically undoubtedly have more diverse chromatic tuning than do LGN neurons (Gegenfurtner, 2003; Lennie, Krauskopf, & Sclar, 1990; Lennie & Movshon, 2005), and this increased variability has often been taken to support the existence of higher-order psychophysical color mechanisms. Since a very large number of different lights – not to mention surfaces – can be discriminated in color (Krauskopf & Gegenfurtner, 1992; MacAdam, 1947), there must be different neurons at some level of the brain that are tuned to many different color directions, at least at the moment the discrimination is made. The question is how the activity of those cells is reflected in the behavior of the observer, and whether the mechanism concept is useful in summarizing that relationship.

A great deal of evidence, from a very broad range of good psychophysical experiments, has supported models with a fairly large number of simple, linear, mechanisms, like the model depicted in Fig. 12, and discredited the simplest, cardinal axis model such as shown in Fig. 1. However, it remains to be seen whether a model with fewer, more complex and nonlinear mechanisms, such as the RGIDBY model of Fig. 13, could account for the detection as well as discrimination results – once a consensus on the results themselves can be reached.

Acknowledgments

I am grateful to Thorsten Hansen and Andrew Stockman for insightful comments on a draft of this paper, and to Karl Gegenfurtner and an anonymous reviewer for challenging me to improve it.

References

Ahumada, A. J. Jr., (2002). Classification image weights and internal noise level estimation. *Journal of Vision, 2*, 121–131. Available from http://journalofvision.org/2/1/8/.

Atick, J. J., Li, Z., & Redlich, A. N. (1993). What does post-adaptation color appearance reveal about cortical color representation? *Vision Research, 33*, 123–129.

Bouet, R., & Knoblauch, K. (2004). Perceptual classification of chromatic modulation. *Visual Neuroscience, 21*, 283–289.

Boynton, R. M. (1979). *Human color vision*. New York: Holt, Rinehart, and Winston.

Boynton, R. M., & Kambe, N. (1980). Chromatic difference steps of moderate size measured along theoretically critical axes. *Color Research and Application, 5*, 13–23.

Boynton, R. M., Nagy, A. L., & Olson, C. X. (1983). A flaw in equations for predicting chromatic differences. *Color Research and Application, 8*, 69–74.

Calkins, D. J., Thornton, J. E., & Pugh, E. N. Jr., (1992). Monochromatism determined at a long-wavelength/middle-wavelength cone-antagonistic locus. *Vision Research, 32*, 2349–2367.

Cardinal, K. S., & Kiper, D. C. (2003). The detection of colored glass patterns. *Journal of Vision, 3*, 199–208. Available from http://journalofvision.org/3/3/2/.

Chaparro, A., Stromeyer, C. F., 3rd., Chen, G., & Kronauer, R. E. (1995). Human cones appear to adapt at low light levels: Measurements on the red–green detection mechanism. *Vision Research, 35*, 3103–3118.

[6] There are counterexamples: it is generally believed there are only two or three temporal channels in photopic vision (Hess & Plant, 1985; Mandler & Makous, 1984), for example.

Chaparro, A., Stromeyer, C. F., 3rd., Kronauer, R. E., & Eskew, R. T. Jr., (1994). Separable red–green and luminance detectors for small flashes. *Vision Research, 34*, 751–762.

Clifford, C. W., Spehar, B., Solomon, S. G., Martin, P. R., & Zaidi, Q. (2003). Interactions between color and luminance in the perception of orientation. *Journal of Vision, 3*, 106–115. Available from http://journalofvision.org/3/2/1/.

Cole, G. R., Hine, T., & McIlhagga, W. (1993). Detection mechanisms in L-, M-, and S-cone contrast space. *Journal of the Optical Society of America A, 10*, 38–51.

Cole, G. R., Stromeyer, C. F., 3rd., & Kronauer, R. E. (1990). Visual interactions with luminance and chromatic stimuli. *Journal of the Optical Society of America A, 7*, 128–140.

Dakin, S. C. (1997). The detection of structure in glass patterns: Psychophysics and computational models. *Vision Research, 37*, 2227–2246.

De Valois, R. L., & De Valois, K. K. (1993). A multi-stage color model. *Vision Research, 33*, 1053–1065.

Derrington, A. M., Krauskopf, J., & Lennie, P. (1984). Chromatic mechanisms in lateral geniculate nucleus of macaque. *The Journal of Physiology, 357*, 241–265.

D'Zmura, M. (1991). Color in visual search. *Vision Research, 31*, 951–966.

D'Zmura, M., & Knoblauch, K. (1998). Spectral bandwidths for the detection of color. *Vision Research, 38*, 3117–3128.

Eskew, R. T. Jr., (1989). The gap effect revisited: Slow changes in chromatic sensitivity as affected by luminance and chromatic borders. *Vision Research, 29*, 717–729.

Eskew, R. T. Jr., (2008). Chromatic detection and discrimination. In R. H. Masland & T. D. Albright (Eds.). *The senses: A comprehensive reference* (Vol. 2: Vision II, pp. 101–117). New York: Academic Press.

Eskew, R. T., Jr., & Giulianini, F. (2005). Nonlinear cone combination in *S* cone mechanisms: Results that are independent of color representation and off-axis looking [Abstract]. *Journal of Vision, 5*, 25a. Available from http://journalofvision.org/5/12/25/.

Eskew, R. T., Jr., & Kortick, P. M. (1994). Hue equilibria compared with chromatic detection in 3D cone contrast space. *Investigative Ophthalmology & Visual Science, 35*(Suppl), 1554.

Eskew, R. T., Jr., McLellan, J. S., & Giulianini, F. (1999). Chromatic detection and discrimination. In K. R. Gegenfurtner & L. T. Sharpe (Eds.), *Color vision: From genes to perception* (pp. 345–368). Cambridge: Cambridge University Press.

Eskew, R. T., Jr., Newton, J. R., & Giulianini, F. (2001). Chromatic detection and discrimination analyzed by a Bayesian classifier. *Vision Research, 41*, 893–909.

Eskew, R. T., Jr., Stromeyer, C. F., 3rd., Picotte, C. J., & Kronauer, R. E. (1991). Detection uncertainty and the facilitation of chromatic detection by luminance contours. *Journal of the Optical Society of America A, 8*, 394–403.

Eskew, R. T., Jr., Stromeyer, C. F., 3rd., & Kronauer, R. E. (1994). Temporal properties of the red–green chromatic mechanism. *Vision Research, 34*, 3127–3137.

Eskew, R. T., Jr., Wang, Q., & Richters, D. P. (2003). Colour detection, discrimination, and hue in the (*S*, *M*) and (*S*, *L*) planes of colour space. *Perception, 32*(Suppl.), 39.

Flanagan, P., Cavanagh, P., & Favreau, O. E. (1990). Independent orientation-selective mechanisms for the cardinal directions of colour space. *Vision Research, 30*, 769–778.

Fletcher, H. (1940). Auditory patterns. *Review of Modern Physics, 12*, 47–65.

Gegenfurtner, K. R. (2003). Cortical mechanisms of colour vision. *Nature Reviews Neuroscience, 4*, 563–572.

Gegenfurtner, K. R., & Kiper, D. C. (1992). Contrast detection in luminance and chromatic noise. *Journal of the Optical Society of America A, 9*, 1880–1888.

Giulianini, F., & Eskew, R. T. Jr., (1998). Chromatic masking in the ($\Delta L/L$, $\Delta M/M$) plane of cone-contrast space reveals only two detection mechanisms. *Vision Research, 38*, 3913–3926.

Giulianini, F., & Eskew, R. T. Jr., (2007). Theory of chromatic noise masking applied to testing linearity of *S*-cone detection mechanisms. *Journal of the Optical Society of America A, 24*, 2604–2621.

Goda, N., & Fujii, M. (2001). Sensitivity to modulation of color distribution in multicolored textures. *Vision Research, 41*, 2475–2485.

Gowdy, P. D., Stromeyer, C. F., 3rd., & Kronauer, R. E. (1999). Facilitation between the luminance and red–green detection mechanisms: Enhancing contrast differences across edges. *Vision Research, 39*, 4098–4112.

Graham, N. V. S. (1989). *Visual pattern analyzers*. New York: Oxford University Press.

Gulick, W. L., Gescheider, G. A., & Frisina, R. D. (1989). *Hearing: Physiological acoustics, neural coding, and psychoacoustics*. New York: Oxford.

Gunther, K. L., & Dobkins, K. R. (2003). Independence of mechanisms tuned along cardinal and non-cardinal axes of color space: Evidence from factor analysis. *Vision Research, 43*, 683–696.

Hansen, T., & Gegenfurtner, K. R. (2005). Classification images for chromatic signal detection. *Journal of the Optical Society of America A, 22*, 2081–2089.

Hansen, T., & Gegenfurtner, K. R. (2006). Higher level chromatic mechanisms for image segmentation. *Journal of Vision, 6*, 239–259. Available from http://journalofvision.org/5/12/25/.

Harnad, S. (1987). Introduction: Psychophysical and cognitive aspects of categorical perception: A critical overview. In S. Harnad (Ed.), *Categorical perception: The groundwork of cognition*. Cambridge: Cambridge University Press.

Hess, R. F., & Plant, G. T. (1985). Temporal frequency discrimination in human vision: Evidence for an additional mechanism in the low spatial and high temporal frequency region. *Vision Research, 25*, 1493–1500.

Hurvich, L. M., & Jameson, D. (1957). An opponent-process theory of color vision. *Psychological Review, 64, Part 1*(6), 384–404.

Knoblauch, K. (1995). Dual bases in dichromatic color space. In B. Drum (Ed.), *Colour vision deficiencies XII*. Dordrecht: Kluwer Academic.

Knoblauch, K., & D'Zmura, M. (2001). Reply to letter to editor by M. J. Sankeralli, & K. T. Mullen published in Vision Research, 41, 53–55: Lights and neural responses do not depend on choice of color space. *Vision Research, 41*, 1683–1684.

Krauskopf, J. (1999). Higher order color mechanisms. In K. R. Gegenfurtner & L. T. Sharpe (Eds.), *Color vision: From genes to perception* (pp. 303–316). Cambridge: Cambridge University Press.

Krauskopf, J., & Gegenfurtner, K. (1992). Color discrimination and adaptation. *Vision Research, 32*, 2165–2175.

Krauskopf, J., Williams, D. R., & Heeley, D. W. (1982). Cardinal directions of color space. *Vision Research, 22*, 1123–1131.

Krauskopf, J., Williams, D. R., Mandler, M. B., & Brown, A. M. (1986). Higher order color mechanisms. *Vision Research, 26*, 23–32.

Krauskopf, J., Wu, H. J., & Farell, B. (1996). Coherence, cardinal directions and higher-order mechanisms. *Vision Research, 36*, 1235–1245.

Krauskopf, J., Zaidi, Q., & Mandler, M. B. (1986). Mechanisms of simultaneous color induction. *Journal of the Optical Society of America A, 3*, 1752–1757.

Laming, D. (1973). *Mathematical psychology*. London: Academic.

LeGrand, Y. (1949/1994). *Form and space vision*. Bloomington, IN: Indiana University Press.

Lennie, P., & D'Zmura, M. (1988). Mechanisms of color vision. *Critical Reviews in Neurobiology, 3*, 333–400.

Lennie, P., Krauskopf, J., & Sclar, G. (1990). Chromatic mechanisms in striate cortex of macaque. *Journal of Neuroscience, 10*, 649–669.

Lennie, P., & Movshon, J. A. (2005). Coding of color and form in the geniculostriate visual pathway (invited review). *Journal of the Optical Society of America A, 22*, 2013–2033.

Li, A., & Lennie, P. (1997). Mechanisms underlying segmentation of colored textures. *Vision Research, 37*, 83–97.

Lindsey, D. T., & Brown, A. M. (2004). Masking of grating detection in the isoluminant plane of DKL color space. *Vision Neuroscience, 21*, 269–273.

Lindsey, D. T., Pokorny, J., & Smith, V. C. (1986). Phase-dependent sensitivity to heterochromatic flicker. *Journal of the Optical Society of America A, 3*, 921–927.

MacAdam, D. L. (1942). Visual sensitivities to color differences in daylight. *Journal of the Optical Society of America, 32*, 247–274.

MacAdam, D. L. (1947). Note on the number of distinct chromaticities. *Journal of the Optical Society of America, 37*, 308–309.

MacLeod, D. I. A., & Boynton, R. M. (1979). Chromaticity diagram showing cone excitation by stimuli of equal luminance. *Journal of the Optical Society of America, 69*, 1183–1186.

Mandler, M. B., & Makous, W. (1984). A three channel model of temporal frequency perception. *Vision Research, 24*, 1881–1888.

McGraw, P. V., McKeefry, D. J., Whitaker, D., & Vakrou, C. (2004). Positional adaptation reveals multiple chromatic mechanisms in human vision. *Journal of Vision, 4*(7), 626–636.

McKeefry, D. J., McGraw, P. V., Vakrou, C., & Whitaker, D. (2004). Chromatic adaptation, perceived location, and color tuning properties. *Visual Neuroscience, 21*, 275–282.

McLellan, J. S., & Eskew, R. T. Jr., (2000). ON and OFF S-cone pathways have different long-wave cone inputs. *Visual Research, 40*, 2449–2465.

Mizokami, Y., Paras, C., & Webster, M. A. (2004). Chromatic and contrast selectivity in color contrast adaptation. *Visual Neuroscience, 21*, 359–363.

Mollon, J. D., & Cavonius, C. R. (1987). The chromatic antagonisms of opponent process theory are not the same as those revealed in studies of detection and discrimination. In G. Verriest (Ed.). *Colour vision deficiencies* (Vol. VIII, pp. 473–483). Dordrecht: Junk.

Monaci, G., Menegaz, G., Susstrunk, S., & Knoblauch, K. (2004). Chromatic contrast detection in spatial chromatic noise. *Visual Neuroscience, 21*, 291–294.

Monnier, P., & Nagy, A. L. (2001). Uncertainty, attentional capacity and chromatic mechanisms in visual search. *Vision Research, 41*, 313–328.

Mullen, K. T., & Kulikowski, J. J. (1990). Wavelength discrimination at detection threshold. *Journal of the Optical Society of America A, 7*, 733–742.

Nagy, A. L., Neriani, K. E., & Young, T. L. (2004). Color mechanisms used in selecting stimuli for attention and making discriminations. *Visual Neuroscience, 21*, 295–299.

Newton, J. R., & Eskew, R. T. Jr., (2003). Chromatic detection and discrimination in the periphery: A postreceptoral loss of color sensitivity. *Visual Neuroscience, 20*, 511–521.

Polden, P. G., & Mollon, J. D. (1980). Reversed effect of adapting stimuli on visual sensitivity. *Proceedings of the Royal Society of London. Series B, 210*, 235–272.

Pugh, E. N., Jr., & Kirk, D. B. (1986). The pi mechanisms of W S Stiles: An historical review. *Perception, 15*, 705–728.

Pugh, E. N., Jr., & Mollon, J. D. (1979). A theory of the $\pi 1$ and $\pi 3$ color mechanisms of Stiles. *Vision Research, 19*, 293–312.

Rodieck, R. W. (1973). *The vertebrate retina*. San Francisco: W.H. Freeman.

Sankeralli, M. J., & Mullen, K. T. (1996). Estimation of the L-, M-, and S-cone weights of the postreceptoral detection mechanisms. *Journal of the Optical Society of America A, 13*, 906–915.

Sankeralli, M. J., & Mullen, K. T. (1997). Postreceptoral chromatic detection mechanisms revealed by noise masking in three-dimensional cone contrast space. *Journal of the Optical Society of America A, 14*, 2633–2646.

Sankeralli, M. J., & Mullen, K. T. (2001). Assumptions concerning orthogonality in threshold-scaled versus cone-contrast colour spaces. *Vision Research, 41*, 53–55.

Sankeralli, M. J., Mullen, K. T., & Hine, T. J. (2002). Ratio model serves suprathreshold color-luminance discrimination. *Journal of the Optical Society of America A, 19*, 425–435.

Shimono, K., Shioiri, S., & Yaguchi, H. (2009). Psychophysical evidence for a purely binocular color system. *Vision Research, 49*(2), 202–210.
Shinomori, K., Spillmann, L., & Werner, J. S. (1999). S-cone signals to temporal OFF-channels: Asymmetrical connections to postreceptoral chromatic mechanisms. *Vision Research, 39*, 39–49.
Stiles, W. S. (1949). Increment thresholds and the mechanisms of colour vision. *Documenta Ophthalmologia, 3*, 138–165.
Stiles, W. S. (1978). *Mechanisms of colour vision*. London: Academic Press.
Stockman, A., & Brainard, D. H. (in press). Color vision mechanisms. In M. Bass, C. DeCusatis, J. Enoch, V. Larkshminarayanan, G. Li, C. Macdonald, V. Mahajan, & E. van Stryland (Eds.), *The optical society of America handbook of optics volume III: Vision and vision optics* (3rd ed.). New York: McGraw Hill.
Stockman, A., & Plummer, D. J. (2005). Spectrally opponent inputs to the human luminance pathway: Slow +L and −M cone inputs revealed by low to moderate long-wavelength adaptation. *Journal of Physiology, 566*(Pt 1), 77–91.
Stockman, A., Plummer, D. J., & Montag, E. D. (2005). Spectrally opponent inputs to the human luminance pathway: Slow +M and −L cone inputs revealed by intense long-wavelength adaptation. *Journal of Physiology, 566*(Pt 1), 61–76.
Stromeyer, C. F., 3rd., Chaparro, A., Rodriguez, C., Chen, D., Hu, E., & Kronauer, R. E. (1998). Short-wave cone signal in the red–green detection mechanism. *Vision Research, 38*, 813–826.
Stromeyer, C. F., 3rd., Chaparro, A., Tolias, A. S., & Kronauer, R. E. (1997). Colour adaptation modifies the long-wave versus middle-wave cone weights and temporal phases in human luminance (but not red–green) mechanism. *Journal of Physiology, 499*, 227–254.
Stromeyer, C. F., 3rd., & Lee, J. (1988). Adaptational effects of short wave cone signals on red–green chromatic detection. *Vision Research, 28*, 931–940.
Stromeyer, C. F., 3rd., Thabet, R., Chaparro, A., & Kronauer, R. E. (1999). Spatial masking does not reveal mechanisms selective to combined luminance and red–green color. *Vision Research, 39*, 2099–2112.
Swanson, W. H., Ueno, T., Smith, V. C., & Pokorny, J. (1987). Temporal modulation sensitivity and pulse-detection thresholds for chromatic and luminance perturbations. *Journal of the Optical Society of America A, 4*, 1992–2005.
Thornton, J. E., & Pugh, E. N. Jr., (1983). Red/green opponency at detection threshold. *Science, 219*, 191–193.
Watson, A. B., & Robson, J. G. (1981). Discrimination at threshold: Labelled detectors in human vision. *Vision Research, 21*, 1115–1122.
Webster, M. A., Malkoc, G., Bilson, A. C., & Webster, S. M. (2002). Color contrast and contextual influences on color appearance. *Journal of Vision, 2*, 505–519. Available from http://journalofvision.org/2/6/7/.
Webster, M. A., & Mollon, J. D. (1991). Changes in colour appearance following post-receptoral adaptation. *Nature, 349*, 235–238.
Webster, M. A., & Mollon, J. D. (1994). The influence of contrast adaptation on color appearance. *Vision Research, 34*, 1993–2020.
Webster, M. A., & Wilson, J. A. (2000). Interactions between chromatic adaptation and contrast adaptation in color appearance. *Vision Research, 40*, 3801–3816.
Whitaker, D., McGraw, P. V., & Levi, D. M. (1997). The influence of adaptation on perceived visual location. *Vision Research, 37*, 2207–2216.
Wilson, J. A., & Switkes, E. (2005). Integration of differing chromaticities in early and midlevel spatial vision. *Journal of the Optical Society of America A, 22*, 2169–2181.
Wuerger, S. M., Atkinson, P., & Cropper, S. (2005). The cone inputs to the unique-hue mechanisms. *Vision Research, 45*, 3210–3223.
Zaidi, Q. (2001). Is there a perceptual color space? Book review of R. D. Luce, M. D'Zmura, D. Hoffman, G. J. Iverson, & A. K. Romney (Eds.) (1995), Geometric representations of perceptual phenomena. C*olor Research and Application, 26*(4), 325–328.
Zaidi, Q., & Halevy, D. (1993). Visual mechanisms that signal the direction of color changes. *Vision Research, 33*, 1037–1051.
Zaidi, Q., & Shapiro, A. G. (1993). Adaptive orthogonalization of opponent-color signals. *Biological Cybernetics, 69*, 415–428.
Zaidi, Q., Shapiro, A., & Hood, D. (1992). The effect of adaptation on the differential sensitivity of the S-cone color system. *Vision Research, 32*, 1297–1318.